1 Spatial and temporal dynamics of suspended sediment concentrations in coastal waters of South
2 China Sea, off Sarawak, Borneo: Ocean colour remote sensing observations and analysis

3 **Jenny Choo[1], Nagur Cherukuru[2], Eric Lehmann[2], Matt Paget[2], Aazani Mujahid[3], Patrick Martin[4], Moritz Müller[1]**

4 [1]Swinburne University of Technology, Faculty of Engineering, Computing and Science, Jalan Simpang Tiga, 93350 Kuching,
5 Sarawak, Malaysia.
6 [2]Commenwealth Scientific and Industrial Research Organization (CSIRO), Canberra ACT 2601, Australia.
7 [3]Faculty of Resource Science & Technology, University Malaysia Sarawak, Kota Samarahan 94300, Sarawak, Malaysia.
8 [4]Asian School of the Environment, Nanyang Technological University, 639798, Singapore.
9
10 *Correspondence to*: Jenny Choo (JChoo@swinburne.edu.my/jccy89@gmail.com)

12 Abstract

13 High-quality ocean colour observations are increasingly accessible to support various monitoring and
14 research activities for water quality measurements. In this paper, we present a newly developed
15 regional total suspended solids (TSS) empirical model using MODIS-Aqua's Rrs(530) and Rrs(666)
16 reflectance bands to investigate the spatial and temporal variation of TSS dynamics along the
17 southwest coast of Sarawak, Borneo. The performance of this TSS retrieval model was evaluated using
18 error metrics (bias = 1.0, MAE = 1.47, and RMSE = 0.22 in mg/L) with a log10 transformation prior to
19 calculation, as well as a k-fold cross validation technique. The temporally averaged map of TSS
20 distribution, using daily MODIS-Aqua satellite datasets from 2003 until 2019, revealed large TSS
21 plumes detected particularly in the Lupar and Rajang coastal areas on a yearly basis. The average TSS
22 concentration range of 15 – 20 mg/L was estimated at these coastal areas. Moreover, the spatial map
23 of TSS coefficient of variation (CV) indicated strong TSS variability (approximately 90 %) in the
24 Samunsam-Sematan coastal areas, which could potentially impact nearby coral reef habitats in this
25 region. Our findings on temporal TSS variation provide further evidence that monsoonal patterns drive
26 the TSS release in these tropical water systems, with distinct and widespread TSS plume variations
27 observed between the northeast and southwest monsoon periods. Map of relative TSS distribution
28 anomalies revealed strong spatial TSS variations in the Samunsam-Sematan coastal areas, while 2010
29 recorded a major increase (approximately 100 %) and widespread TSS distribution with respect to the
30 long-term mean. Furthermore, our findings on the contribution of river discharge to the TSS
31 distribution showed a weak correlation across time at both the Lupar and Rajang river mouth points.
32 The variability of TSS distribution across coastal river points was studied by investigating the variation
33 of TSS pixels at three transect points, stretching from the river mouth into territorial and open water
34 zones, for eight main rivers. Our findings showed a progressively decreasing pattern of nearly 50 % in
35 relation to the distance from shore, with exceptions in the northeast regions of the study area.
36 Essentially, our findings demonstrate that the TSS levels at the southwest coast of Sarawak are within
37 local water quality standards, promoting various marine and socio-economic activities. This study
38 presents the first observation of TSS distributions at Sarawak coastal systems with the application of
39 remote sensing technologies, to enhance coastal sediment management strategies for the sustainable
40 use of coastal waters and their resources.

41 Keywords: total suspended solids, band-ratio, monsoon, river discharge, Open Data Cube

1.0 Introduction

Total Suspended Solids (TSS) play an important role in the aquatic ecosystem as one of the primary water quality indicators of coastal and riverine systems (Alcântara et al., 2016; Cao et al., 2018; Chen et al., 2015a; González Vilas et al., 2011; Mao et al., 2012). For example, elevated concentrations of TSS in water have an adverse impact on fisheries and biodiversity of the aquatic ecosystem (Bilotta and Brazier, 2008; Chapman et al., 2017; Henley et al., 2000; Wilber and Clarke, 2001). Understanding the impacts of varying water quality in relation to TSS status has been one of the primary concerns with respect to a country's growing Blue Economy status and sustainable management of aquatic resources (Lee et al., 2020a; Sandifer et al., 2021; World Bank and United Nations Department of Economic and Social Affairs (UNDESA), 2017). With about 40 % of the world's population living within 100 km of coastal areas (United Nations, 2017), and with more than 80 % of the population in Malaysia living within 50 km of the coast (Praveena et al., 2012), water quality monitoring and management efforts are important at both regional and global scale.

Studying TSS distribution can provide insights into the connections between land and ocean ecosystems (Howarth, 2008; Lemley et al., 2019; Lu et al., 2018). For instance, TSS dynamics allow us to understand the impacts of sediment transport and sediment plumes, particularly in areas experiencing large-scale deforestation, land conversion and damming of rivers (Chen et al., 2007; Espinoza Villar et al., 2013). Sarawak, Malaysian Borneo, experienced significant land use and land cover change activities over the past four decades, with widespread land conversion and deforestation for developments and large-scale plantation activities (Gaveau et al., 2016), as well as building of major road infrastructures, such as the Pan-Borneo highway, and hydroelectric dams (Alamgir et al., 2020). As a result, river and coastal systems may potentially drive large TSS loads into downstream systems and into the marine and open ocean waters.

Situated at the southern part of the South China Sea, the region of Sarawak, Malaysian Borneo, has a coastline of about 1035 km where mangrove forests are dominant (Long, 2014). The

70   coastal regions of Sarawak are rich with marine coastal biodiversity and coral reefs, which can be

71   found at the northeast and southwest part of Sarawak (Praveena et al., 2012). While the coasts of

72   Sarawak provide important socio-economic values to the local communities (Lee et al., 2020b), these

73   coastal areas are potentially facing water quality degradation from TSS riverine outputs in response

74   to land use and land cover change activities.

75   TSS concentrations are commonly measured through conventional laboratory-based methods

76   to quantify TSS concentrations by field collection of water samples (Ling et al., 2016; Mohammad Razi

77   et al., 2021; Soo et al., 2017; Soum et al., 2021; Tromboni et al., 2021; Zhang et al., 2013). Currently,

78   real-time high-frequency TSS observations using modern optical and bio-sensor systems are also

79   possible (Bhardwaj et al., 2015; Horsburgh et al., 2010). These sensors can be generally found onboard

80   ship and buoy-based observation platforms. Yet, it remains a challenge to quantify TSS concentrations

81   of large spatial coverage and high temporal frequency with these approaches.

82   Ocean colour remote sensing technologies represent an increasingly accessible and powerful

83   tool to provide a synoptic view for short or long-term water quality studies at high temporal and spatial

84   resolutions (Cherukuru et al., 2016a; Slonecker et al., 2016; Swain and Sahoo, 2017; Wang et al., 2017;

85   Werdell et al., 2018). Remote sensing can help overcome several constraints of conventional intensive

86   field campaigns such as: (i) costly field campaigns from boat rentals or cruise; (ii) time-consuming and

87   inadequate manpower; and most importantly for this study, (iii) limited spatial and temporal field

88   coverage. NASA's Moderate Resolution Imaging Spectroradiometer (MODIS)-Aqua

89   (https://modis.gsfc.nasa.gov/about/) has a distinctive advantage with its daily revisit time, a spatial

90   resolution of 250 – 1000 m, and a large collection of ocean colour data since 2002. Other sensors

91   offering ocean colour measurement capabilities include Landsat-8, which, in comparison with MODIS-

92   Aqua, has a 16-day revisit time and high spatial resolution of 30 m. Despite Landsat's powerful ability

93   in capturing higher resolution images, the longer revisit interval may not be suitable for characterizing

94   and studying water bodies with high dynamics of various water constituents.

95   Several MODIS-derived models have been developed for TSS retrievals (Chen et al., 2015b;

96   Espinoza Villar et al., 2013; Jiang and Liu, 2011; Kim et al., 2017; Zhang et al., 2010b), including

97   empirical, semi-analytical and machine-learning approaches (Balasubramanian et al., 2020; Jiang et

98   al., 2021). However, the performance of these models proved to be less satisfactory, with recorded

99   low r^2 and high bias and mean absolute error (MAE) values when tested with in situ TSS datasets

100   (Supplementary Materials, Table S1). While these global TSS remote sensing models address the need

101   to improve TSS retrievals and to monitor global TSS trends in various water class types, they tend to

102   underperform in more localised and regional studies (Mao et al., 2012; Ondrusek et al., 2012). The

103   coastal waters of Borneo are well-mixed throughout the year and enriched with suspended material

104   and dissolved organic matter (Müller et al., 2016). Various water quality studies of the river systems

105   have been actively carried out to assess the dynamics of numerous water quality constituents in

106   response to human activities, with TSS concentrations being one of the primary environmental

107   concerns in this region (Ling et al., 2016; Müller-dum et al., 2019; Tawan et al., 2020). Although studies

108   on the water quality of coastal systems in Borneo have gradually gained much attention (Cherukuru

109   et al., 2021; Limcih et al., 2010; Martin et al., 2018; Soo et al., 2017), there is still much knowledge to

110   gain on the understanding of how coastal waters in the region have been impacted by TSS loadings

111   and transport over large spatial and temporal scales.

112   Here, in this paper, we present a new regional empirical TSS remote sensing model. While

113   various remote sensing models have their own unique computational strengths, this paper

114   demonstrates the reliability of band ratio TSS model to be applied within optically complex waters.

115   With the ongoing efforts to address and minimize water quality degradation in coastal systems, as

116   outlined in the United Nation's Sustainability Development Goals no. 14, our study aims to apply the

117   new empirical regional TSS remote sensing model to: (a) investigate the spatial and temporal

118   variability in TSS, (b) identify hotspots of TSS distribution in the coastal waters of Sarawak, Malaysian

119   Borneo, using a long time series of MODIS-Aqua data from year 2003 until 2019, and (c) study the

120   varying monsoonal and river discharge patterns in relation to TSS distribution at river mouths.

121   2.0 Methodologies

122   Figure below summarizes the processes carried out in this study. Spatial and temporal variation of TSS

123   distribution was mapped using atmospheric-corrected MODIS-Aqua Level 2 product.

124
125   Existing in situ TSS measurements from Martin et al. (2018) and spectral reflectance data from Cherukuru et al. (2021)

126

127
128   Development of regional TSS remote sensing model

129   Validation of TSS remote sensing model performance via statistical analysis

130
131   Application of TSS remote sensing model on Open Data Cube (ODC) platform

132

133   Retrieval of atmospheric-corrected MODIS-Aqua Level 2 product in ODC platform

134

135
136   Retrieval of Global Precipitation Measurement (GPM) datasets

137   Computation of river discharge using GPM datasets

138

139
140   Map and plot daily MODIS-Aqua satellite datasets from 2003 till 2019 on:

141   • Spatial variation of TSS
       • Temporal variation of TSS
142   • Relationship between TSS and river discharge
       • TSS variability across coastal waters
143

Fig. 1: Flowchart summarizing the processes of developing a regional TSS remote sensing model and applying it to analyse the spatial and temporal variation of TSS over the study region, using MODIS-Aqua data from year 2003 until 2019. Long-term MODIS-Aqua datasets were analysed and mapped on an Open Data Cube (ODC) platform with implementation of robust Python libraries and packages.

2.1 Area of study

Our study focuses on the southwestern coast of Sarawak (between 1.9° N, 109.65° E and 2.8° N, 111.5° E) in Malaysia, which sits at the northwest part of the Borneo Island. Generally, the island of Borneo (between 3.01° S, 112.18° E and 6.45° N, 117.04° E) contains rich tropical rainforests and biodiversity on the lands of Sarawak and Sabah (Malaysia), Brunei, and Indonesia. Typically, Sarawak is a tropical climate region, recording an average ambient temperature of 27.8 °C (variation of 1.8 °C) throughout the year. It records high precipitation with an average of 4116.7 mm/yr in Kuching (1.5535° N, 110.3593° E), the capital city of Sarawak. Yearly, it experiences both a dry and wet season, which is influenced by: (i) the southwestern monsoon (May to September) and (ii) the northeastern monsoon (November to March). Rivers in Sarawak are connected to the South China Sea and flow through various plantation types, such as oil palm, rubber and sago (Davies et al., 2010).

In this study, we studied the southwestern part of Sarawak's coastal regions (Fig. 2), (between 1.9° N, 109.65° E and 2.8° N, 111.5° E), which comprise several major rivers (e.g. Lupar, Sebuyau, Sematan), as well as the Rajang River, the longest river in Malaysia. These river systems are associated with increasing land use activities and land cover changes in this region, which essentially transport and connect various biogeochemical water components to the coastal systems of Sarawak.

165

Fig. 2: Map of the study area (© Google Maps), located in the southwestern part of Sarawak, Malaysia (inset). Indicators

show the location of sampling sites used during field expeditions carried out in June and September 2017.

2.2 In situ TSS measurements

TSS measurements data were taken from Martin et al. (2018). A total of 35 coastal sites were studied

and are denoted SJ, SS, and SM (see: Table 1 & Fig. 2). These water samples were collected in the

month of June (SJ region) and September (SS and SM regions) in 2017. Water samples were filtered,

and filters were dried and ashed prior to weighing process. Full details of water sampling and TSS

analysis is available in Martin et al. (2018).

2.3 Development, calibration and validation of TSS model

In situ remote sensing reflectance spectral data, Rrs(λ), along with 35 measured TSS values, were used

to develop a new remote sensing TSS empirical model for MODIS-Aqua for this case study. Field

177   measurements of SM, SJ & SS datasets, as shown in Table 1, were used to calibrate the MODIS-Aqua

178   TSS remote sensing model.

179   For the in situ remote sensing reflectance, Rrs(λ) readings, a TriOS-RAMSES spectral imaging

180   radiometer was used to measure downwelling irradiance, Ed(λ), and upwelling radiance, Lu(λ), with

181   measurement protocols from Mueller et al. (2002). These measurements were recorded under stable

182   sky and sea conditions during the day (10AM to 4PM) with high-sun elevation angle condition.

183   Measurements of reflectance, Rrs(λ), were recorded concurrently with the collection of water samples

184   (as described in Section 2.2) and were recorded at wavelength ranging from 280 to 950 nm, which

185   covers the spectrum of ultraviolet, visible and visible/ultraviolet light. These measurements were

186   recorded on a float to capture Lu(0−, λ) and Ed(0+, λ), where 0- and 0+ refer to below-surface and

187   above-surface, respectively.

188   Remote sensing reflectance, Rrs(λ), was computed as follows with reference to Mueller et al. (2002):

$$Rrs(\lambda, 0+) = \frac{1-p}{n^2} \times \frac{Lu(0-,\lambda)}{Ed(0+,\lambda)} \qquad (1)$$

189   where p = 0.021 refers to the Fresnel reflectance and n =1.34 is the refractive index of water. Full

190   details of this methodology can be found at Cherukuru et al. (2021).

191   2.3.1 Calibration of empirical model and application to MODIS-Aqua

192   With the intention to apply regional TSS remote sensing model to MODIS-Aqua product, a total

193   number of 35 TSS datasets were collected in coastal conditions (salinity > 15 PSU) and convolved to

194   generate MODIS-Aqua data.

195   In this study, retrieval of water constituents was established using spectral band ratio combinations

196   which have proven to be a straightforward, yet reliable method for estimating water constituents in

197   optically turbid waters (Ahn and Shanmugam, 2007; Cao et al., 2018; Lavigne et al., 2021; Morel and

198   Gentili, 2009; Neil et al., 2019; Siswanto et al., 2011). Band ratio models help to offset signal noise,

199 such as the effects of atmospheric and irradiance of spectral reflectance to a certain degree

200 (Cherukuru et al., 2016b; Ha et al., 2017; Hu et al., 2012; Liu et al., 2019).

201 A variety of models using single bands, as well as a combination of MODIS-Aqua's Blue, Green & Red

202 bands (412nm, 440nm, 488nm, 532nm, 555nm & 660nm) were calibrated using field measurements

203 as dependent variable. The calibration process was tested out using various model functions, including

204 linear, power, exponential, and logarithm functions. The best empirical TSS retrieval model was fitted

205 by means of a regression between the in situ TSS data and in situ radiometer values, and can be

206 expressed as follows:

207 $$TSS = 21.238[Rrs(530)/Rrs(666)]^{-1.272} \qquad (2)$$

208 This power function model resulted in a coefficient of determination (R^2) of 0.82 (Fig. 3).

209 Table 1: Summary statistics of TSS values collected at areas SJ, SS, and SM located within coastal regions in this study, with a
210 total of 35 datasets recorded.

Coastal Area	Minimum	Maximum	Mean	S.D.	C.V.	n
SJ	1.1	19.24	6.89	6.62	96.09	6
SS	0.56	32.1	12.50	11.43	91.45	16
SM	0.5	8.14	2.59	2.70	104.53	13

211
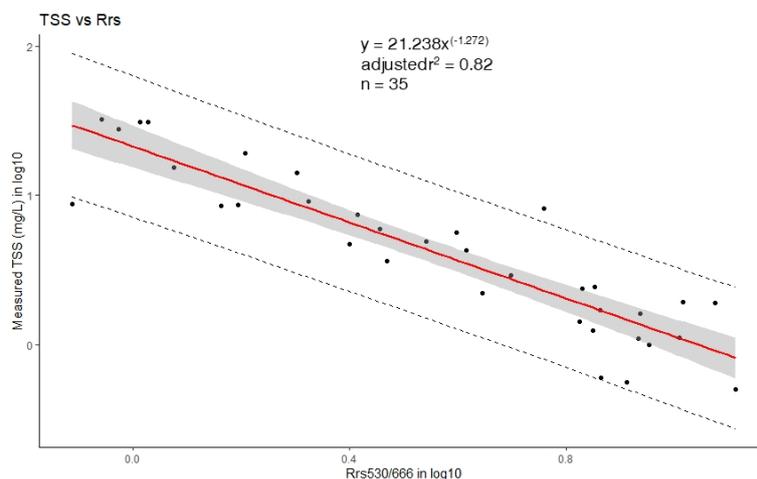
212

213   Fig. 3: Empirical relationship of TSS retrieval between in situ Rrs(530)/Rrs(666) bands ratio and measured TSS
214   concentration (mg/L), as established via a power law function. Upper and lower dashed lines indicate the 95 % prediction
215   interval of the regression.

216   2.3.2 Performance assessment and validation of MODIS-Aqua empirical model

217   An evaluation of the model was performed using a k-fold cross validation technique (Refaeilzadeh et

218   al., 2020) given the small size of the TSS dataset used in this study (Table 2). A selection of k = 7 was

219   assigned to split the datasets into k groups with an equal number of data points.

220   An assessment of the performance error of the newly developed TSS model was carried out as per

221   Seegers et al. (2018)'s recommendation for interpreting ocean colour models. These performance

222   metrics used here include the bias, Mean Absolute Error (MAE), Root Mean Squared Error (RMSE),

223   coefficient of variation (CV), as well as the coefficient determination, r^2, based on the following

224   calculations:

225    $$\text{Bias} = 10^{\wedge} \left[\frac{\sum_{i=1}^{n} log10\ (Mi) - log10(Oi)}{n} \right] \qquad (3)$$

226    $$\text{MAE} = 10^{\wedge} \left[\frac{\sum_{i=0}^{n} |\ log10\ (Mi) - log10(Oi)\ |}{n} \right] \qquad (4)$$

227    $$\text{RMSE} = \sqrt{\frac{\sum_{i=1}^{n} (log10(Mi) - log10(Oi))^{\wedge}2}{n}} \qquad (5)$$

228    $$\text{CV} = \frac{\sigma}{\mu} \times 100\% \qquad (6)$$

229   where M represents the modelled TSS values, n is the number of samples, and O represents the

230   observed TSS measurements, while σ refers to standard deviation and μ represents the mean value.

231   Equation (3), (4) and (5) use a log10-transform of the data as the range of TSS values can span several

232   orders of magnitude. As such, an application of the log-transform prior to error metric calculation

233   allows us to account for uncertainties that are proportional to the concentration values

234   (Balasubramanian et al., 2020; Seegers et al., 2018).

235   Table 2: Assessment of fitting error for the proposed TSS model, using k-fold cross validation.

Parameter	k-fold (n)	R2	RMSE	MAE
TSS	7	0.85	0.2159	0.1747

236

237 Table 3: Calibration and accuracy assessment of the newly derived MODIS-Aqua models in this study for TSS estimations.
238 Calculation for bias, MAE and RMSE use a log-transform of the data prior to calculation of error metric measurements, as
239 adapted from Seegers et al. (2018) and Balasubramanian et al. (2020).

Parameter	Bands (nm)	Model	Bias	MAE	RMSE	CV (%)	R
TSS	Rrs(530), Rrs(666)	TSS = 21.238[(Rrs530/Rrs 666)]^-1.272	0.9999	1.4732	0.2161	4.74	0.84

240
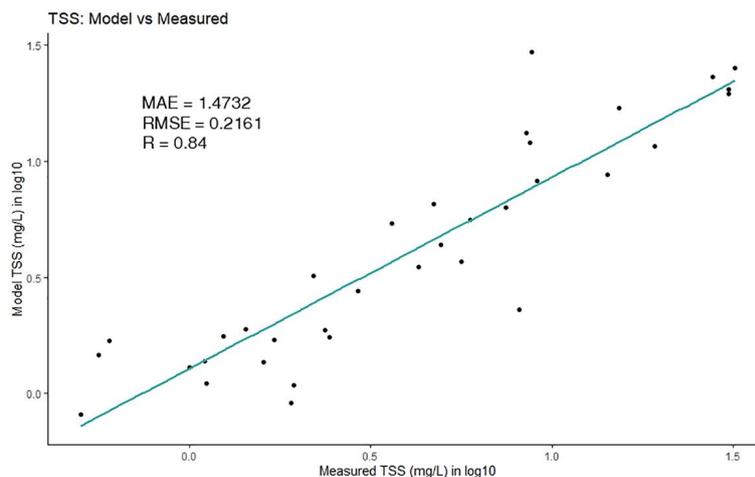
241

242 Fig. 4: Scatterplot of modelled TSS values derived from the proposed model and measured TSS values (mg/L). Check
243 decimals in figure

244 While these results point to low error levels achieved by the proposed regional TSS retrieval model

245 (Table 3, Fig. 4), caution should be used when applying it to various water types. Water type

246 classification has been thoroughly described by Balasubramanian et al. (2020) where waters are

247 classed into Type I (Blue-Green waters), Type II (Green waters), and Type III (Brown waters).

248 Essentially, the Green-to-Red band ratio is optimised with these datasets corresponding to sediment-

249 dominated and yellow-substance loaded water conditions. As highlighted by Morel & Belanger (2006),

250 this type of waters is not spectrally consistent to phytoplankton-rich waters (also known as Case 1

251 waters). In addition to the impact on water clarity, sediment particles (often red-brownish coloured)

252 also tend to enhance the backscattering and absorption properties, especially at shorter wavelengths

253 (Babin et al., 2003), while the additional presence of coloured dissolved matter (yellow substance)

254   leads to strong absorption properties at short wavelengths. As the TSS retrieval model was developed

255   from samples taken in waters that are bio-optically rich in suspended solids and dissolved organic

256   matter, an application of this TSS model needs to be done cautiously when applying to other water

257   types, particularly those with large concentration of phytoplankton.

258   2.4 Application of TSS retrieval model

259   Daily MODIS-Aqua satellite data from year 2003 to 2019 (total of 6192 individual time slices) were

260   studied with a 2°x 2° spatial resolution (longitude: 109.38, 112.0; latitude: 1.22, 3.35) which covers

261   the southwestern coastal region of Sarawak and southern part of the South China Sea.

262   Atmospherically corrected MODIS-Aqua level 2 reflectance products (Bailey et al., 2010; NASA Official,

263   n.d.) were retrieved for the application of the TSS model proposed in this study. Negative remote

264   sensing reflectance values, possibly due to failure of atmospheric correction, were filtered out before

265   applying the retrieval model, as expressed in Eq. (2), to map the spatial and temporal distribution of

266   TSS estimates. In addition, averaging of spatial and temporal TSS variation maps in this study was

267   carried out by filtering TSS values with fewer than 10 valid data points over the whole time series,

268   along with application of sigma clipping operation

269   (https://docs.astropy.org/en/stable/api/astropy.stats.sigma_clip.html)

270   2.4.1 Open Data Cube

271   In this study, the analysis of remote sensing data over large spatial extents and at high temporal

272   resolution was carried out using robust Python libraries and packages run on an Open Data Cube (ODC)

273   platform. Open Data Cube is an open-source advancement in computing technologies and data

274   architectures which addresses the growing volume of freely available Earth Observation (EO) satellite

275   products (Giuliani et al., 2020; Killough, 2019). ODC provides a collection of software which index,

276   manage, and process large EO datasets such as satellite products from the MODIS, Landsat and

277   Sentinel missions (Gomes et al., 2021). These satellite datasets are structured in a multi-dimensional

278   array format, and provide layers of information across latitude and longitude (Open Data Cube, 2021).

279   Leveraging the growing availability of Analysis Ready Data (ARD), and with support from the

280   Committee of Earth Observation Satellites (CEOS) (Killough, 2019), the ODC concept has been

281   deployed in many countries across the world. These existing deployments include Digital Earth Africa

282   (https://www.digitalearthafrica.org/), Digital Earth Australia (DEA) (https://www.dea.ga.gov.au/),

283   Vietnam Open Data Cube (http://datacube.vn/), and Brazil Data Cube (https://github.com/brazil-data-

284   cube), which provide various time-series datasets of the changing landscape and water content in

285   these specific regions (Giuliani et al., 2020; Gomes et al., 2021; Killough, 2019; Lewis et al., 2017). The

286   ecosystem and architecture of ODC is well explained at opendatacube.org. The codes and tools used

287   in this application drew upon the information provided in various DEA notebooks (Krause et al. (2021),

288   which can be found at https://github.com/GeoscienceAustralia/dea-notebooks/.

289   2.5 Computation of river discharge

290   Derivation of river discharge (m^3/s) was computed using total precipitation estimates (mm) over each

291   river basin, and multiplied by a surface discharge runoff factor for the studied region (Sim et al., 2020).

292   The surface runoff was estimated to be 60 % of total precipitation (Staub et al., 2000; Whitmore,

293   1984). Precipitation data were extracted from the monthly NASA Global Precipitation Measurement

294   (GPM) Level 3 IMERG dataset (https://gpm.nasa.gov/data/imerg). In this study, the Rajang river basin,

295   as well as the combined basins of the Lupar, Sadong, and Saribas rivers (hereafter referred to as the

296   Lupar basin), were studied for their river discharge rates in relation to TSS release.

297

298

299

300

301

302

303 3.0 Results & Discussion

304 3.1 Spatial variation of TSS distribution

305 Changes in TSS distribution occur across space and time. The regional TSS remote sensing model

306 calibrated in this study was applied to the time series of MODIS-Aqua data to study the variability of

307 spatial TSS distribution and identify potential hotspot areas susceptible to TSS water quality

308 degradation. The map of average TSS for the Sarawak region was generated (Eq. 2) by averaging all

309 the daily MODIS-Aqua TSS images (2003 to 2019) and is presented in Fig. 5. The results show that the

310 waters in the northeast of the study area, stretching from the Sadong river to the Rajang/Igan river

311 have seen sustained levels of TSS over the 17 years considered in this study.

312 The temporally average spatial distribution map (Fig. 5) shows TSS concentrations in the range of 15

313 – 20 mg/L near the river mouth areas, with widespread TSS plumes extending into the South China

314 Sea (Fig. 5). Based on the Malaysia Marine Water Quality Criteria and Standard (Supplementary

315 Materials, Table S2) (Department of Environment, 2019), these coastal waters fall under Class 1 in

316 relation to their TSS (mg/L) status. This classification indicates that these coastal waters support and

317 preserve marine life in this local region. Yet, several studies have expressed concerns regarding high

318 TSS loadings in riverine waters owing to the impacts of various land use and land cover changes (LULC)

319 (Ling et al., 2016; Tawan et al., 2020). Among these, the Rajang river has been highlighted to be heavily

320 impacted by various LULC activities such as large-scale deforestation and construction of hydropower

321 dams (Alamgir et al., 2020). In situ water quality studies by Ling et al. (2016) reported on high TSS

322 estimates at one of the upstream tributaries of Rajang river, the Baleh river, with TSS readings up to

323 approximately 100 mg/L. Another study by Tawan et al. (2020) reported a significant TSS release

324 reaching to 940,000 mg per day during wet seasons, with maximum TSS concentrations of 1700 mg/L

325 in the upstream tributaries of the Rajang river, particularly at the Baleh and Pelagus rivers. The

326 majority of the upstream tributary rivers were categorised as Class II (during dry season) and Class III

327 (during wet season) waters according to the National Water Quality Index (Supplementary Materials,

328 Table S3) (Department of Environment, 2014), due to increased soil erosion from surrounding LULC

329 activities (Tawan et al., 2020). These local in situ findings provide valuable insights on point source TSS

330 estimates in these LULC change regions. Coupled with our spatial map of average TSS captured by

331 remote sensing technologies, our findings seem to suggest that a large portion of TSS loadings from

332 inland and upstream rivers would have settled and deposited in these river channels and were not

333 completely discharged outwards into the coastal areas, which would have caused major water quality

334 degradation in the corresponding coastal systems.
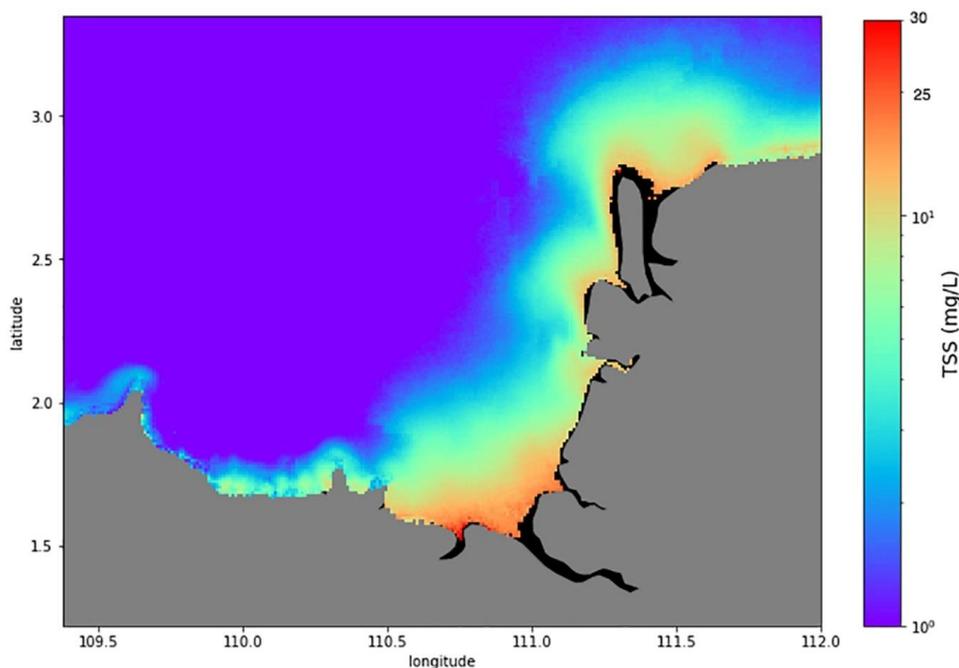
335

336 Fig. 5: Temporally averaged 2°x 2° map of TSS distribution (on a log scale) across the time dimension for each pixel.

337 Historical patterns of TSS concentration were assessed by comparing annual maps of average TSS

338 distribution (Supplementary Materials; Fig. S1), as well as time series of TSS estimates at the Lupar

339 and Rajang river mouths (Supplementay materials; Fig. S2). From our findings, the annual TSS maps

340 further support the observation where TSS release was evident at Lupar and Rajang/Igan river mouths

341 from 2003 till 2019, which points to Class I of local water quality standards in relation to TSS (mg/L)

342   status. This was found to consistently occur every year. Furthermore, the TSS trend study showed that

343   both the Lupar and Rajang river mouth points have a gradual increase of TSS concentration over the

344   17 years (Supplementay materials; Fig. S2). This increasing trend was, however, not statistically

345   significant (p = 0.43 for Lupar, and p = 0.15 for Rajang).

346   Moreover, a map of the TSS coefficient of variation (CV) was computed to identify areas with a high

347   degree of relative TSS variation over time (Fig. 6). Here again, the map of CV (%) was produced by

348   aggregation of the daily MODIS-Aqua images (6192 time steps) from 2003 until 2019. Figure 6 shows

349   that the Samunsam-Sematan coastal region (as highlighted by the red box) exhibits an increased level

350   of TSS distribution variability, with a recorded CV of more than 90 %.

351   The Samunsam-Sematan coastal region contains near-pristine mangrove forests which are sheltered

352   from major LULC activities, as compared to other studied sites. Samunsam-Sematan is also well-known

353   locally as a recreational hotspot with coral reefs and various national parks (Sarawak Tourism Board,

354   2021). Data from the Centre for International Forestry Research (CIFOR) Forrest Carbon database

355   (CIFOR, n.d.) revealed that there was more than double the amount of total forest loss (approx. 5,000

356   Ha) recorded in Lundu, a nearby township in the Sematan area in 2011 as compared to the previous

357   years. Deforestation activities, regardless of their scale, can inevitably promote sediment loss and soil

358   leaching into the nearby river systems (Yang et al., 2002). Important information regarding the

359   variability in water quality (as shown in Fig. 6) can provide support to local authorities and relevant

360   agencies in order to identify vulnerable areas that need to be monitored closely, such as the Lundu-

361   Sematan region in this case. The CV map thus offers interesting insights into how TSS distribution can

362   vary across large spatial areas, which can ultimately impact local socio-economic activities in this

363   region (Lee et al., 2020b).
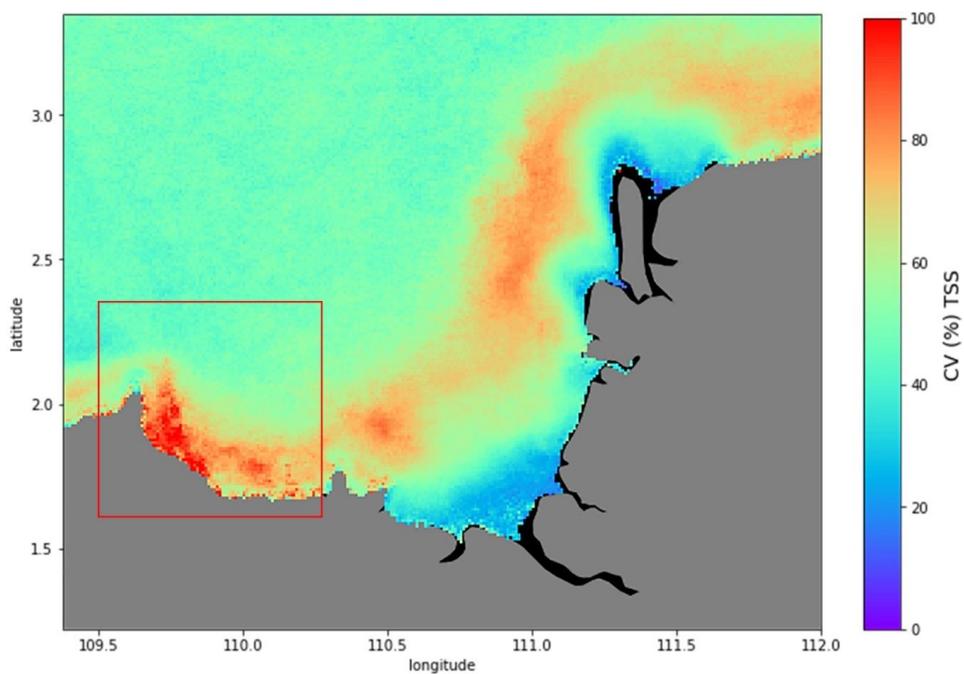
364

365   Fig. 6: Map of CV (%) calculated from the daily time series of MODIS-Aqua satellite images from 2003 until 2019.

366

367

368

369

370

371

372

373

374

375

376   3.2 Temporal variation of TSS distribution

377   On a temporal scale, the northeast (NE) monsoon period shows a distinct difference in the widespread

378   intensity of TSS distribution as compared to the southwest (SW) monsoon period, along the Sarawak

379   coastline over the 17 years of the considered time series (Fig. 7). Mapping of temporal variations

380   between monsoons using time-series MODIS-Aqua datasets can provide an improved understanding

381   on the intensity of monsoonal patterns in driving the TSS distribution in this region. As shown in Figure

382   7, TSS release can be seen to extend further into the open ocean South China Sea region during the

383   NE monsoon periods (Fig. 7a) in comparison to the SW monsoon periods (Fig. 7b).

384   In addition, the differences in TSS release between the NE and SW monsoons ((NE-SW)/NE x 100) were

385   mapped as shown in Fig. 7c. Widespread TSS plumes are detected at Lundu/Sematan region (>80 %

386   relative difference in TSS concentration) on the southwest side of the study area, while substantial

387   TSS plumes are observed in front of the Igan river channel, with more than 50 % relative difference in

388   TSS concentration in comparison to SW monsoon periods. Sadong coastal area is observed to receive

389   considerable TSS loadings (> 30%) during NE monsoon periods.

390   These coastal areas would thus be more likely to be impacted by the TSS release during the NE

391   monsoon periods. These findings further strengthen the evidence that tropical rivers are majorly

392   impacted by climatic variability such as monsoonal patterns, as highlighted in a study at Baleh river in

393   Sarawak (Chong et al., 2021). This suggests that monsoon rains, which typically last for several months,

394   play an integral role in driving the discharge of TSS in tropical rivers.

395

396

397

398

399

400

401
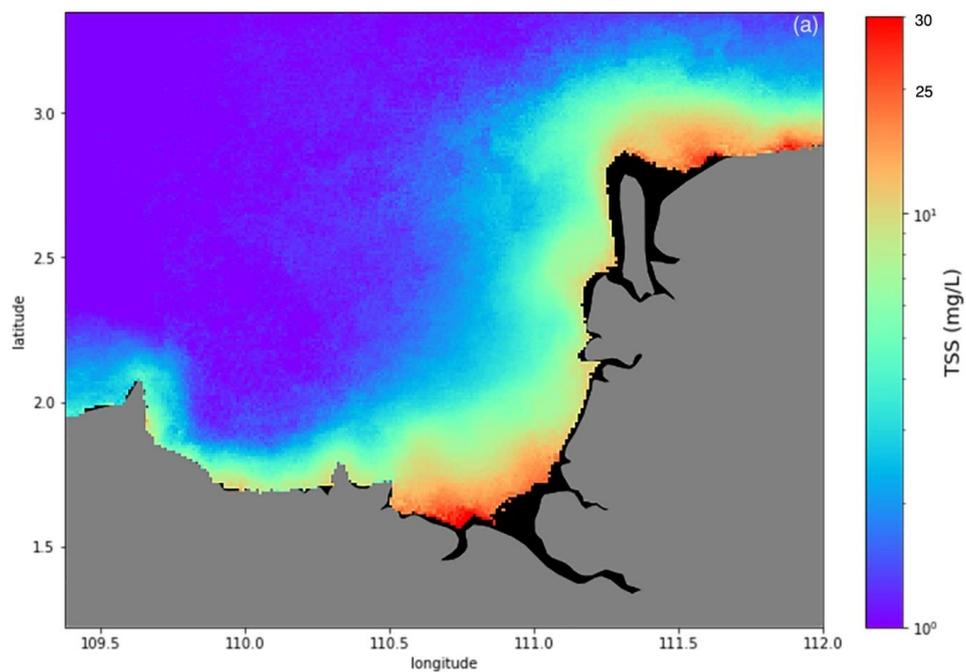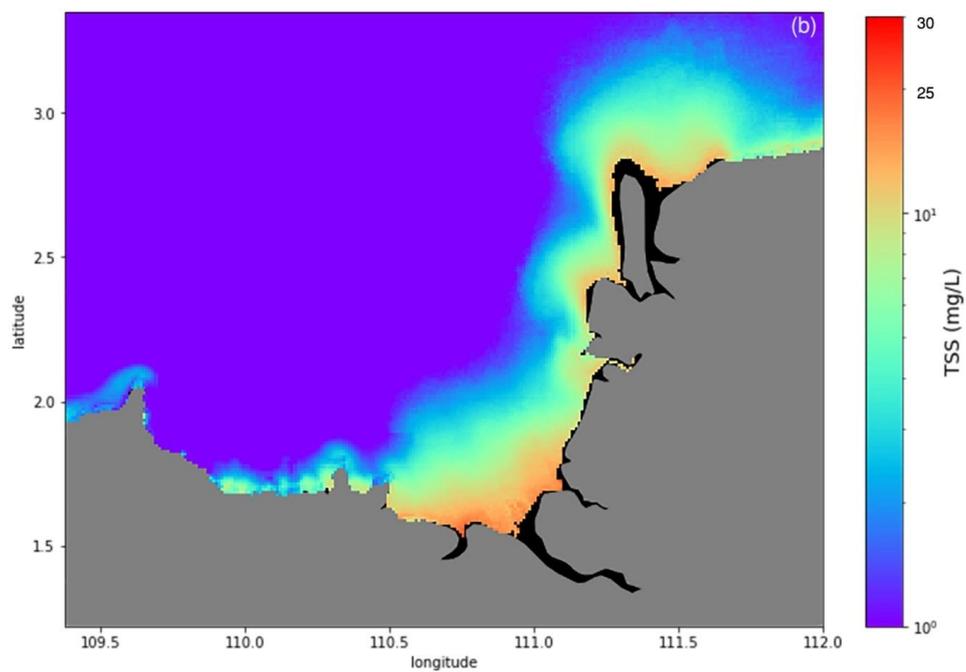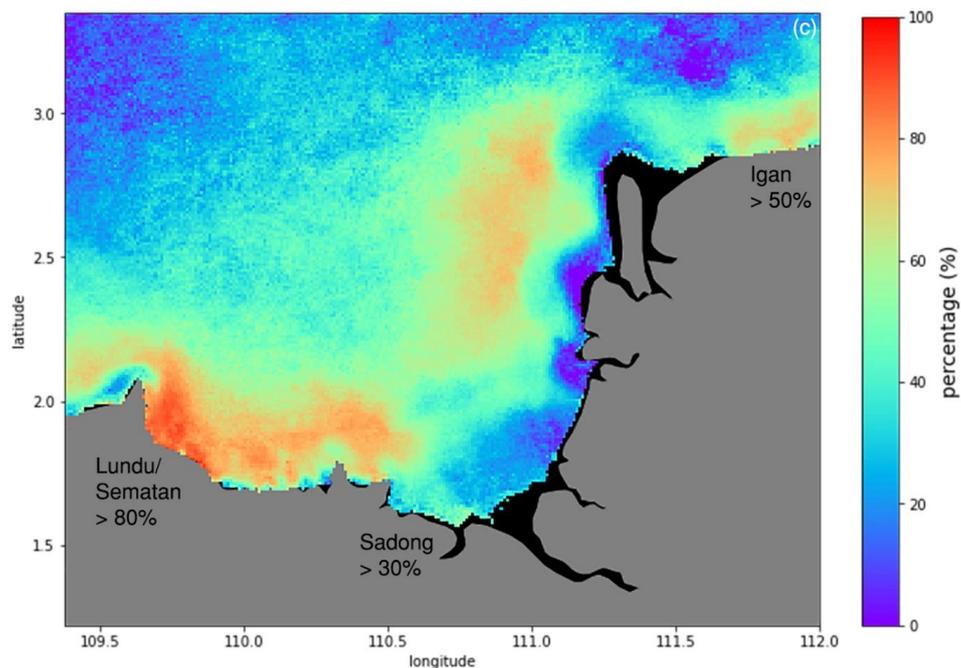
Fig. 7: Long-term average of TSS estimates (mg/L) during the Northeast monsoon (a), and the Southwest monsoon (b). The

map of TSS difference between the Northeast and Southwest monsoon periods, computed in relative percentage (%), is

shown in (c).

405   Several climatic studies in the Borneo region highlighted 2009 as a year with extreme rainfall events

406   which caused major floods in Sarawak (Dindang et al., 2011; Sa'adi et al., 2017), while drought events

407   were reported in 2014 (Bong and Richard, 2020). Hence, in this study, TSS dynamics for the Lupar and

408   Rajang rivers were studied by assessing the variation of TSS values at selected pixels in relation to

409   monsoonal rainfall patterns in 2009 and 2014 (Supplementary Materials; Fig. S3).

410   Monthly precipitation values (mm) over the Lupar and Rajang basins were extracted from the Global

411   Precipitation Measurement (GPM) satellite datasets (Supplementary Materials, Fig. S4 - 7) in order to

412   assess the influence of precipitation in each river basin in relation to TSS concentration at the

413   corresponding river mouth.

414   Generally, the results show fluctuations of TSS concentrations across the NE and SW monsoon periods

415   in relation to precipitation values (Fig. 8a – d). Based on Fig. 8a, monthly precipitation values recorded

416   for the Lupar river basin in 2009 showed a clear decreasing trend from the NE monsoon period (wet

417   season) to the SW monsoon period (dry season), while gradually increasing approaching the year end's

418   NE monsoonal period. A similar precipitation pattern was observed for the Rajang river basin during

419   the same year (Fig. 8c).

420   However, these results also show that the TSS distribution (mg/L) at the Lupar river mouth seems to

421   show no distinct trend of decreasing TSS concentration estimates during the SW monsoon period in

422   year 2009 (Fig. 8a) in relation to its precipitation values. Additionally, a sharp rise of TSS release can

423   be seen in the month of May (beginning of SW monsoon period), with a near equivalent intensity of

424   TSS release during the NE monsoon period. This observation may potentially be caused by the lag

425   between the time of rainfall events occurring during NE monsoon periods and TSS release entering

426   the coastal river regions. A similar observation was described by Sun et al. (2017a) suggesting that

427   riverine outputs could take several days, and even up to one month to reach the coastal river points.

428   Considering the occurrence of extreme rainfall events in 2009, our findings are in agreement with

429   these processes as TSS concentrations generally exhibit a similar intensity throughout the NE and SW

430   monsoonal periods for the Lupar river (Fig. 8a). This result could suggest that the occurrence of

431   extreme rainfall events, as reported for the year 2009, can exert a much larger impact on TSS

432   transportation and release in monsoon-driven tropical rivers.

433   However, our estimates show a generally lower TSS concentration at the Rajang river mouth during

434   the SW monsoon periods (dry season) in 2009 (Fig. 8c) as compared to the Lupar river mouth (Fig. 8a).

435   While these observations were recorded during the same year in 2009, when Sarawak experienced

436   extreme rainfall events, the monsoonal influence between these two different river basins show a

437   slight difference in terms of TSS distribution. A possible reason for these observations can be explained

438   by the Rajang river's unique meandering features, which can potentially induce a different

439   sedimentological behaviour compared to the Lupar river channels, which was discussed by Omorinoye

440   et al. (2021) in a study on geomorphological features of the Sadong river in relation to the

441   sedimentation process.

442   Drought events in 2014 can be seen to impact the precipitation values at both the Lupar (Fig. 8b) and

443   Rajang river basins (Fig. 8d). There is no apparent patterns of decreasing precipitation values during

444   the shift of NE to SW monsoonal periods as compared to the year 2009, for either river basin. However,

445   precipitation values were found to increase sharply during the year end NE monsoon period for both

446   river basins. The TSS concentrations at the Lupar coastal river points were found to be the highest

447   during the NE monsoon period earlier in January and February of 2014 (Fig. 8b). This may be due to

448   the temporal lag in the transition of TSS discharge into the coastal systems arising from the prior

449   months (November and December) in the previous year, when higher rainfall events were typically

450   observed in this region (Gomyo and Koichiro, 2009; Tangang et al., 2012). The TSS distribution at both

451   Lupar and Rajang coastal river points showed no distinct trend in relation to the precipitation values

452   throughout a period of ten months until November 2014. These findings suggest that coastal areas in

453   the Borneo region may not be experiencing critical water quality degradation during dry seasons.

454

455

456

457

458

459

460

461
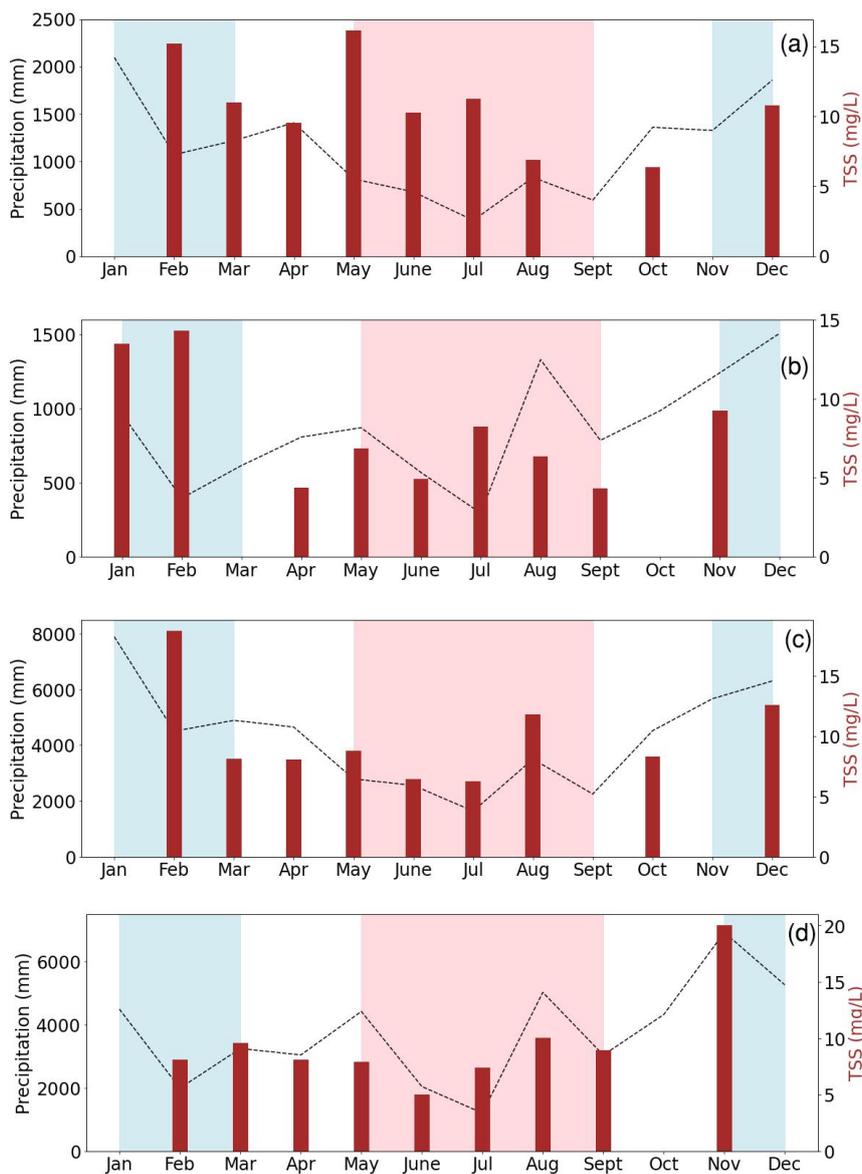
462

463 Fig. 8: Temporal analysis of precipitation (mm) from the Lupar and Rajang river basins in relation to TSS concentrations (mg/L)

464 during the NE and SW monsoon periods at the Lupar ((a): 2009; (c): 2014) and Rajang ((b): 2009; (d): 2014) coastal river point.

465 The NE monsoon months are highlighted with a blue background; those of the SW monsoon with a pink background, and

466 intermonsoon periods with a white background.

467   Considering the temporal variation recorded across monsoons, maps of relative TSS anomalies were

468   calculated for each year as the difference with respect to the long-term TSS mean (Fig. 5), in order to

469   detect changes of TSS distribution occurring annually (Fig. 9). As shown in Figure 9, year 2010

470   experienced a distinct increase of TSS distribution (approximately 100 %), with widespread pattern

471   extending into open ocean waters, in comparison to the long-term TSS mean. This finding provides an

472   interesting insight into the effects of extreme rainfall events as recorded in year 2009, which could

473   potentially intensify TSS release into the coastal and open ocean waters. The effects of TSS release

474   can still be seen a year after the extreme rainfall events in this region. This observation could provide

475   further evidence that the impacts of the TSS release from the land into rivers and coastal systems may

476   only take effect after a substantial period, as previously observed by Sun et al. (2017a).

477   Figure 9 further reveals an interesting pattern of TSS increase in the Samunsam-Sematan region from

478   year 2004 until 2019, with exceptions during the years 2007 and 2008. As previously highlighted in

479   Section 3.1, the Samunsam-Sematan region has been observed to be a vulnerable coastal area with

480   respect to TSS water quality degradation. From the annual map of TSS anomalies (Fig. 9), we can see

481   that the TSS distribution has the tendency to accumulate in the Samunsam-Sematan region, as

482   opposed to being distributed into the open ocean waters. This may be due to the geographical and

483   hydrological characteristics of these coastal regions (Martin et al., 2018), as the TSS release may be

484   sheltered from open ocean waters, and hence induce a higher TSS accumulation in these coastal

485   regions.

486

487

488

489

490

491
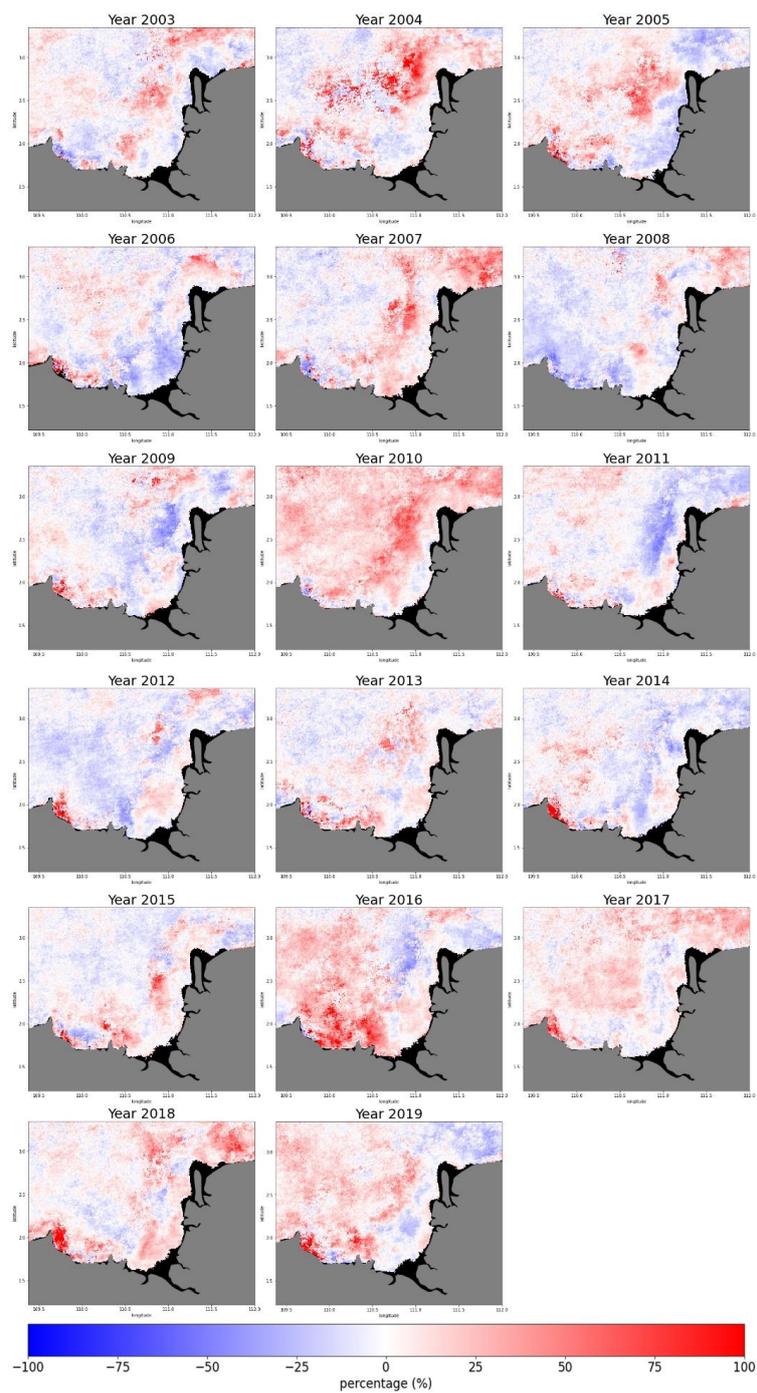
Fig. 9: Map of relative TSS distribution anomalies with respect to the long-term mean, represented as percentage (%), from

493   year 2003 until 2019.

3.3 Hydrological factors driving TSS discharge

Apart from the influence of monsoonal patterns, hydrological factors such as the river discharge are among the dominant drivers in transporting various water constituents in riverine and coastal systems (Loisel et al., 2014; Petus et al., 2014; Sun, 2017b; Verschelling et al., 2017). In this study, river discharge from the Lupar and Rajang basins was estimated and investigated.

Yearly river discharge estimates from 2003 until 2019 were investigated to assess its effect on the TSS distribution (Fig. 10) represented by changes in TSS values for pixels located at each Lupar and Rajang coastal river points (Supplementary Materials, Fig. S3). Figure 10a shows that river discharge values in the Lupar basin (750 to 1050 m³/s) are approximately twice lower than the Rajang river discharge (Fig. 10b), which recorded a range of 3,200 to 4,000 m³/s.

Fig. 10: Time-series analysis of river discharge (m³/s) in relation to TSS concentrations (mg/L) for the Lupar (a) and Rajang (b) basins from year 2003 to 2019. Note the differing scaling on the ordinate axes in each plot.

508   From our findings, discrepancies between TSS estimates and river discharge were identified in both

509   the Lupar and Rajang coastal regions in these annual time-series, where river discharge was inversely

510   correlated with TSS estimates. These discrepancies are not uncommon, as previously highlighted in a

511   study by Zhan et al. (2019). Especially in 2010 for the Lupar river, Fig. 10a shows a drop in TSS release

512   in relation to the steady increase of river discharge from the river basin. In 2011 and 2012, a negative

513   correlation can be seen between river discharge and TSS estimates, while in subsequent years from

514   2013 until 2015, there is a clear positive correlation. Although there is no obvious environmental

515   factor that would explain these discrepancies, these findings may imply a complex interaction

516   between human interventions, such as damming and deforestation activities, as well as varying

517   hydrological and atmospheric conditions (wind and tidal mixing) in regulating TSS dynamics (Wu et al.,

518   2012; Zhan et al., 2019).

519   The correlation between TSS release and river discharge at both the Lupar and Rajang coastal areas

520   was further evaluated in this study. Even though river discharge has been shown (in other global

521   studies) to be one of the dominant factors in moderating TSS release (Fabricius et al., 2016; Tilburg et

522   al., 2015; Verschelling et al., 2017; Wu et al., 2012), the TSS distribution at both the Lupar and Rajang

523   river mouths in this study can be seen to be only poorly correlated with river discharge from each river

524   basin (Supplementary Materials, Fig. S8a and b). The TSS output from the Lupar basin recorded a

525   correlation coefficient of r = 0.15, while river discharge from the Rajang basin did not substantially

526   influence the TSS release either, with r = 0.27 throughout the seasons. Coupled with tidal mixing

527   processes (Ramaswamy et al., 2004; Zhou et al., 2020) , it is possible that human activities such as

528   deforestation, logging, and construction of dams, which are largely occurring within the Rajang basin

529   (Alamgir et al., 2020), are mainly driving TSS release and resuspension in this area. This indicates that

530   although TSS release is regarded to be highly dependent on, and controlled by river discharge patterns,

531   this interaction often represents an intricate process linked to local hydrodynamics process and socio-

532   economic conditions (Espinoza Villar et al., 2013; Fabricius et al., 2016; Valerio et al., 2018; Zhan et al.,

533   2019).

3.4 Variability of TSS across coastal waters

As previously observed in Fig. 5, varying river plumes of TSS were evidently detected within the coastal regions of the study area. Notably, coastal river plumes represent important factors driving the transport of water constituents and nutrients from coastlines to the open oceanic systems (Petus et al., 2014). To assess this and evaluate the water quality status in coastal zones, the spatial extent of TSS release was investigated along transects covering the territorial (12 nautical miles) and open water areas (24 nautical miles) of the Sarawak region (Fig. 11).

A total of eight coastal points were selected based on the main river mouths located in the southwest region of Sarawak. Transect points are positioned in a line starting at the coastal river points to examine the variations of TSS distribution across different water zones. Daily changes in TSS concentration for each pixel located in front of the river mouths were plotted from 2003 until 2019 (Fig. 12).
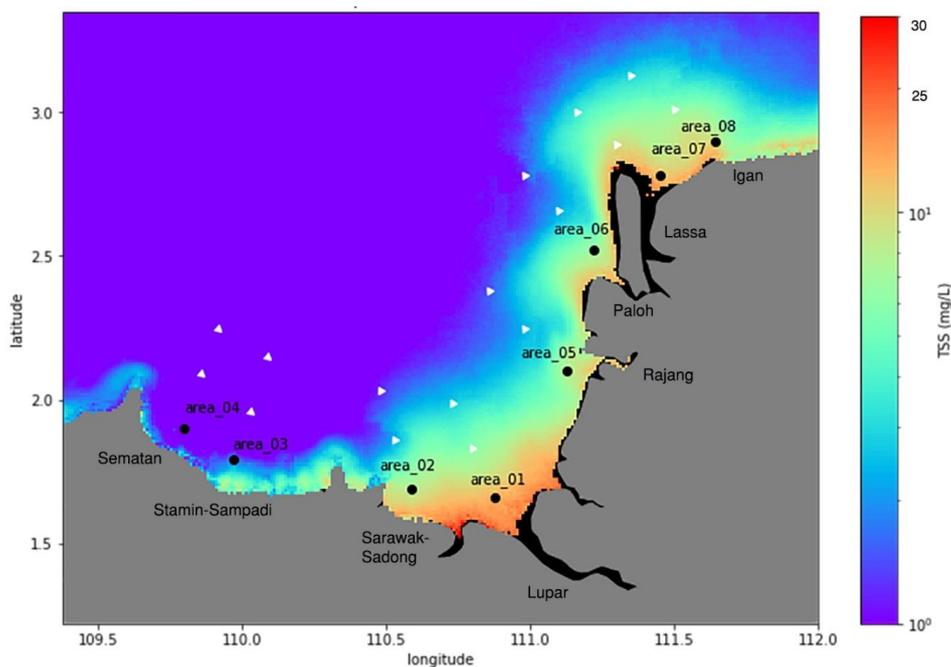
546

547   Fig. 11: Map of average TSS estimates (mg/L) with indicators at eight main river mouths and their transect, extending from

548   coastal waters into territorial and open ocean systems. Indicators of each river mouths are as follows: area_01 – Lupar river;

549   area_02 – Sarawak-Sadong river; area_03 - Stamin-Sampadi river i; area_04 – Sematan river; area_05: Rajang river; area_06:

550   Paloh river; area_07: Lassa river; and area_08: Igan river).

551
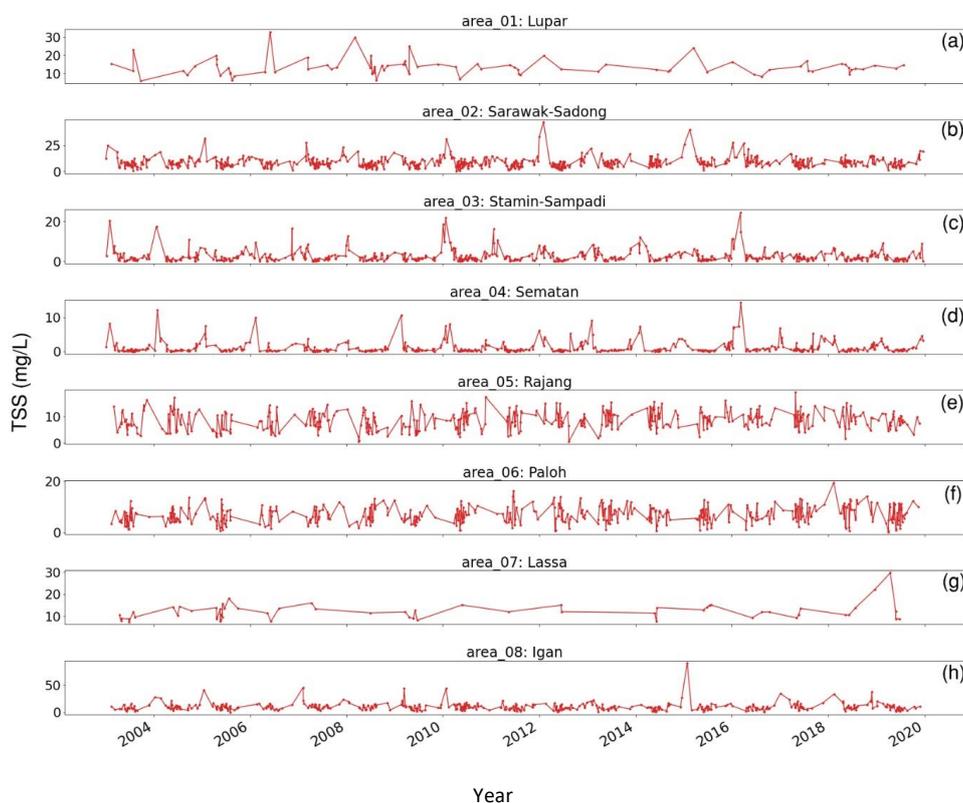
Fig. 12: Graphs of daily TSS estimates (mg/L) recorded at eight river mouth points from 2003 to 2019. Presentation of each

553   river mouths is as follows: a) area_01; b) area_02; c) area_03; d) area_04; e) area_05; f) area_06; g) area_07; h) area_08.

554   Note the different TSS scales in each plot.

555   From the high temporal resolution graphs in Fig. 12, no general trend of TSS concentration can be

556   identified over the years at each coastal point. It is worth highlighting that the daily temporal

557   resolution was particularly affected at coastal points located in front of the Lupar (area_01) and Lassa

558   (area_07) river mouths due to various pixel data quality issues in these areas. Nonetheless, more than

559   80 satellite images with minimum cloud coverage at these two locations were processed, while the

560   remaining coastal points had a total of more than 400 satellite images to assess the temporal trend.

561   Despite the fact that no distinct upward or downward trend was observed, our findings indicate that

562   several river mouths are actively discharging and accumulating substantial TSS amounts over the

563   period of years, while resuspension of bottom sediments induced by wind and tidal cycle is another

564   factor contributing to the variation of TSS values (Park, 2007; Song et al., 2020).

565   The coastal region of the Sarawak-Sadong river (area_02) shows relatively high TSS distribution

566   patterns with some periods recording an estimate of over 30 mg/L of TSS concentration. This is in

567   agreement with the localised characteristics of the Sarawak river basin which essentially drains

568   through the populated Kuching area with high industrial and development activities in the capital city

569   of Sarawak (DID, 2021b). In comparison with other river mouth points, a steady TSS concentration

570   below 20 mg/L was recorded across the Stamin-Sampadi (area_03), Sematan (area_04), Rajang

571   (area_05), and Paloh (area_06) river mouths. Consistently high TSS values in the daily plots were

572   recorded at the Lupar (area_01) and Pulau Bruit-Lassa (area_07) river mouths, with estimates of up to

573   30 mg/L on a near-daily basis. Similar high TSS amounts from the Igan (area_08) river mouth, situated

574   northeast side of the Pulau Bruit-Lassa region, were observed in Cherukuru et al. (2021) and Staub et

575   al. (2000).

576   Although the daily TSS estimates at each river point are in line with various reported studies (Chen et

577   al., 2011, 2015b; Kim et al., 2017; Mengen et al., 2020; Zhang et al., 2010a), these estimates can be

578   expected to be much higher for sampling points much closer to the river mouths. The selection of

579   coastal river points in this study was made to minimize the gaps with respect to various pixel data

580   quality issues in the MODIS-Aqua datasets, and hence, the use of coastal river points closer to shore

581   would have been impractical.

582   These findings further suggest that higher TSS loadings within the coastal river areas would have been

583   diluted or deposited while travelling to the open oceanic systems as they are weakly impacted by river

584   discharge in relation to offshore distance (Espinoza Villar et al., 2013). This understanding can be

585   observed in Fig. 13, which shows a progressively decreasing TSS estimates at each transect in relation

586   to the distance from the shore. Generally, TSS estimates in coastal zones (first transect point) show

587   considerably higher TSS concentrations. When moving outwards to territorial waters (second transect

588   point), TSS concentration estimates decrease by nearly 50 % before travelling to open ocean systems

589   (third transect point), except for the northeast regions (area_07 and area_08) which seem to show

590   large extension of TSS plumes to the open ocean waters, as also highlighted by Cherukuru et al. (2021).

591   A reversed trend can be seen in the plot corresponding to the Sematan coastal river systems, although

592   the absolute increase in TSS estimates across water zones (0.2 mg/L in total) here is only marginal (Fig.

593   15d).

594   Nonetheless, it is important to present these synoptic findings to address existing water quality

595   practices and regulations implemented in this local region, in order to improve the monitoring and

596   management of its coastal systems. According to the Malaysia Marine Water Quality Criteria and

597   Standard (Supplementary Materials, Table S2), the coastal areas of Sarawak are dominantly

598   categorised as Class I quality. Our findings in the southwest coastal areas (Sematan and Stamin-

599   Sampadi) showed that the coral reefs there can be well-maintained with negligible impacts from TSS

600   loadings (Fig. 11). While these Sematan and Stamin-Sampadi coasts can be seen to be in a healthy

601   water quality state (low average TSS concentration, see e.g. Fig 11), the high coefficient variation

602   reported in these coastal waters, as previously highlighted in Section 3.1 (Fig. 6), clearly stresses the

603   importance of understanding how the quality of coastal systems can vary and be affected by human

604   intervention and changing landscapes over time.

605

606

607

608

609

610
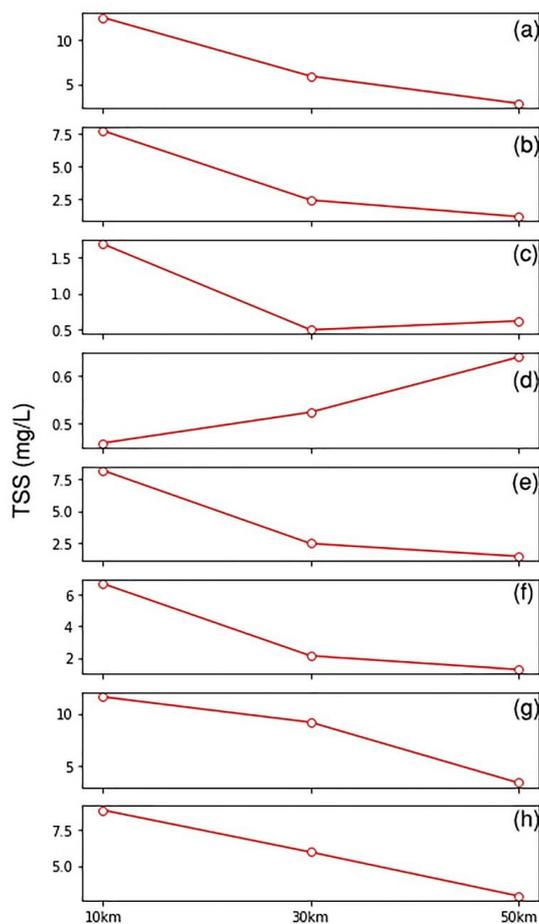
Fig. 13: Average TSS estimates (mg/L) computed from 2003 to 2019 for each of the eight rivers (area_01: (a), area_02: (b);

area_03: (c); area_04: (d); area_05: (e); area_06: (f); area_07: (g); and area_08: (h)) and their relevant transect points with

distance of 10 km (coastal waters), 30 km (territorial waters) and 50 km (open ocean waters) from the shoreline. Note the

varying TSS scales on the ordinate axes in each plot.

615

616

617

618

619 3.5 Discussion of TSS implications for coastal waters

620 High discharge of TSS into coastal environments can lead to adverse environmental and ecological

621 implications. The presence of TSS affects water transparency and light availability within the surface

622 waters (Dogliotti et al., 2015; Nazirova et al., 2021; Wang et al., 2021). Among others, TSS affects the

623 photosynthesis activities of algae and macrophytes. TSS in water creates a reduction in light

624 penetration, which impacts the primary production of aquatic organisms and hence the support

625 system of marine life (Bilotta and Brazier, 2008; Loisel et al., 2014).

626 Additionally, TSS exerts an influence on zooplankton communities. Reduction in water clarity induces

627 changes in the zooplankton's biomass volume and composition, while TSS may carry a level of toxicity

628 which affects zooplankton through ingestion (Chapman et al., 2017; Donohue and Garcia Molinos,

629 2009). Apart from that, accumulation and deposition of sediments decreases the level of dissolved

630 oxygen (DO) at the bottom of the water column, and subsequently impacts the benthic invertebrate

631 groups (Chapman et al., 2017). Moreover, substantial TSS deposition tends to cause harmful physical

632 effects to these benthic groups, such as abrasion, and even clogging by sediment particles (Chapman

633 et al., 2017; Langer, 1980).

634 As a result of these TSS effects on lower trophic levels, fish communities are critically impacted, with

635 a reduction in diversity and abundance (Kemp et al., 2011). While fish communities learn to adapt to

636 a range of TSS loads (Macklin et al., 2010), increase of TSS concentrations often depletes DO

637 concentrations in the water system and causes stress towards these aquatic communities (Henley et

638 al., 2000). Fish populations tend to decrease, as feeding and growth rates are negatively impacted

639 (Shaw and Richardson, 2001; Sutherland and Meyer, 2007).

640 Threats to coral reefs have been linked to sediment-induced stress which often leads to a reduction

641 in the coral's growth and metabolic rate, as well as impending mortality (Erftemeijer et al., 2012;

642 Gilmour et al., 2006; Risk and Edinger, 2011). Factors of coral stress are driven by nutrient-rich

643 sediments and microbes which are being carried by TSS, with impacts on the health of coral tissues

644   (Hodgson, 1990; Risk and Edinger, 2011; Weber et al., 2006). A reduction in light availability impede

645   the development of corals (Anthony and Hoegh-Guldberg, 2003; Rogers, 1979; Telesnicki and

646   Goldberg, 1995). A combined increase in TSS and nutrient loadings contribute to the decrease of coral

647   species diversity and composition (Fabricius, 2005).

648   Essentially, presence of TSS in water systems has impacts across various aquatic biota. With the severe

649   implications of decreased fish population, this could lead to a disruption of fisheries activities by local

650   communities, especially considering that more than 80 % of the Sarawak population is living in the

651   coastal areas (DID, 2021a). Coral reefs are important coastal biodiversity assets to the Sarawak region,

652   especially around the Talang-Talang and Satang islands on the southwest coast of Sarawak (Long,

653   2014). With the use of remote sensing technologies in monitoring Sarawak coastal water quality, the

654   approach presented in this paper provides digital-based solutions to assist relevant authorities and

655   local agencies to better manage the Sarawak coastal waters and their resources.

656

657

658

659

660

661

662

663

664

665

666

667

668

669

670   4.0 Conclusion

671   In this study, a regional empirical TSS retrieval model was developed to analyse TSS dynamics along

672   the southwest coast of Sarawak. The empirical relationship between in situ reflectance values, Rrs(λ),

673   and in situ TSS concentrations was established using a green-to-red band ratio using the MODIS-Aqua

674   Rrs(530) and Rrs(666) reflectance bands. An evaluation of the TSS retrieval model was carried out with

675   error metric assessment, which yielded results of bias = 1.0, MAE = 1.47 and RMSE = 0.22 in mg/L

676   computed in log10-transformed space prior to calculation. A statistical analysis using a k-fold cross

677   validation technique (k = 7) reported a low error metrics (RMSE = 0.2159, MAE = 0.1747).

678   The spatial TSS distribution map shows widespread TSS plumes detected particularly in the Lupar and

679   Rajang coastal areas, with average TSS range of 15 – 20 mg/L estimated at these coastal areas. Based

680   on the spatial map of the TSS coefficient of variation, large TSS variability was identified in the

681   Samunsam-Sematan coastal areas (CV > 90 %). The map of temporal variation of TSS distribution

682   points to a strong monsoonal influence in driving TSS release, with large differences identified

683   between the northeast and southwest monsoon periods in this region. From the annual TSS anomalies

684   maps, the Samunsam-Sematan coastal areas demonstrated strong TSS variation spatially, while

685   widespread TSS distribution with nearly 100 % of TSS increase in comparison to long term mean was

686   observed in 2010. Furthermore, our study on river discharge in relation to TSS release demonstrated

687   a weak relationship at both the Lupar and Rajang coastal river points. Study on the TSS variability

688   across coastal river mouths implied that higher TSS loadings in the coastal areas are potentially being

689   deposited or diluted in the process of being transported into the open ocean waters, with varying

690   magnitude at several coastal river points.

691   Overall, these coastal zones remain within local water quality standards to support various marine and

692   socio-economic activities in this region. However, it is important to highlight the various human

693   activities that are widely ongoing in this region, which include deforestation and logging activities

694   (Alamgir et al., 2020; Hon and Shibata, 2013; Vijith et al., 2018). Impacts from these activities in

695   Sarawak can potentially aggravate current soil erosion issues, and ultimately induce more soil leaching

696   and runoff from land to water systems, especially during heavy rainfall events (Ling et al., 2016; Vijith

697   et al., 2018). As a result, human activities may have a greater influence on driving riverine sediments

698   than climatological factors, as reported by Song et al. (2016). As such, this work presents the first

699   observation of TSS distributions at large spatial and temporal scales in Sarawak's coastal systems, and

700   of the potential associated impacts on the South China Sea. The findings derived from this work can

701   be used to support local authorities in assessing TSS water quality status in the coastal areas of

702   concern, and to enhance coastal management and conservation strategies. The application of remote

703   sensing technologies is of great benefit in the development of sustainable sediment management in

704   the Sarawak coastal region, as demonstrated in this study.

705   Data availability. The dataset related to this study is available as supplement to this paper.

706   Author contributions. Conceptualization, J.C., N.C., E.L., and M.M.; Formal analysis, J.C., N.C. and E.L.;

707   Funding acquisition, M.M, N.C., and A.M.; Investigation, J.C., N.C., E.L., M.P., P.M., A.M., and M.M.;

708   Methodology, J.C., N.C., E.L., and M.M.; Resources, J.C., N.C., E.L., M.P., and M.M.; Validation, J.C.,

709   N.C., E.L. and M.M.; Writing— original draft, J.C..; Writing—review & editing, J.C., N.C., E.L., P.M., and

710   M.M.; Supervision, M.M., N.C., and A.M.; Project administration, M.M., A.M., and N.C.

711   Competing interests. The authors declare that they have no conflict of interest.

712   Acknowledgement. We thank Sarawak Forestry Department and Sarawak Biodiversity Centre for

713   permission to conduct collaborative research in Sarawak under permit numbers NPW.907.4.4(Jld.14)-

714   161, SBC-RA-0097-MM, and Park Permit WL83/2017. We would like to extend our gratitude to all the

715   boatmen and crew during all the field expeditions. Special thanks to Pak Mat and Minhad during the

716   western region sampling, and Captain Juble, as well as Lukas Chin, during the eastern region cruises.

717   We are appreciative to members of AQUES MY for their kind participation and involvement, especially

718   to Ashleen Tan, Jack Sim, Florina Richard, Faith Chaya, Edwin Sia, Faddrine Jang, Gonzalo Carrasco,

719   Akhmetzada Kargazhanov, Noor Iskandar Noor Azhar, and Fakharuddin Muhamad. The study was

720   supported by Australian Academy of Sciences under the Regional Collaborations Programme, Sarawak

721   Multimedia Authority (Sarawak Digital Centre of Excellence) and Swinburne University of Technology

722   (Swinburne Research Studentship).

723

724

725

726

727

728

729

730

731

732

733

734

735

736

737

738

739

740

741

742

743

744

745

746

747

748

749

750

751   References:

752   Ahn, Y. and Shanmugam, P.: Derivation and analysis of the fluorescence algorithms to estimate
753   phytoplankton pigment concentrations in optically, , doi:10.1088/1464-4258/9/4/008, 2007.

754   Alamgir, M., Campbell, M. J., Sloan, S., Engert, J., Word, J. and Laurance, W. F.: Emerging challenges
755   for sustainable development and forest conservation in Sarawak, Borneo, PLoS One, 15(3), 1–20,
756   doi:10.1371/journal.pone.0229614, 2020.

757   Alcântara, E., Bernardo, N., Watanabe, F., Rodrigues, T., Rotta, L., Carmo, A., Shimabukuro, M.,
758   Gonçalves, S. and Imai, N.: Estimating the CDOM absorption coefficient in tropical inland waters
759   using OLI/Landsat-8 images, Remote Sens. Lett., 7(7), 661–670,
760   doi:10.1080/2150704X.2016.1177242, 2016.

761   Anthony, K. R. N. and Hoegh-Guldberg, O.: Kinetics of photoacclimation in corals, Oecologia, 134(1),
762   23–31, doi:10.1007/s00442-002-1095-1, 2003.

763   Babin, M., Stramski, D., Ferrari, G. M., Claustre, H., Bricaud, A., Obolensky, G. and Hoepffner, N.:
764   Variations in the light absorption coefficients of phytoplankton , nonalgal particles , and dissolved
765   organic matter in coastal waters around Europe, , 108, doi:10.1029/2001JC000882, 2003.

766   Bailey, S. W., Franz, B. A. and Werdell, P. J.: Estimation of near-infrared water-leaving reflectance for
767   satellite ocean color data processing, Opt. Express, 18(7), 7521, doi:10.1364/oe.18.007521, 2010.

768   Balasubramanian, S. V., Pahlevan, N., Smith, B., Binding, C., Schalles, J., Loisel, H., Gurlin, D., Greb, S.,
769   Alikas, K., Randla, M., Bunkei, M., Moses, W., Nguyễn, H., Lehmann, M. K., O'Donnell, D., Ondrusek,
770   M., Han, T. H., Fichot, C. G., Moore, T. and Boss, E.: Robust algorithm for estimating total suspended
771   solids (TSS) in inland and nearshore coastal waters, Remote Sens. Environ., 246(February), 111768,
772   doi:10.1016/j.rse.2020.111768, 2020.

773   Bhardwaj, J., Gupta, K. K. and Gupta, R.: A review of emerging trends on water quality measurement
774   sensors, Proc. - Int. Conf. Technol. Sustain. Dev. ICTSD 2015, (April), 1–6,
775   doi:10.1109/ICTSD.2015.7095919, 2015.

776   Bilotta, G. S. and Brazier, R. E.: Understanding the influence of suspended solids on water quality and
777   aquatic biota, Water Res., 42(12), 2849–2861, doi:10.1016/j.watres.2008.03.018, 2008.

778   Bong, C. H. J. and Richard, J.: Drought and climate change assessment using standardized
779   precipitation index (Spi) for sarawak river basin, J. Water Clim. Chang., 11(4), 956–965,
780   doi:10.2166/wcc.2019.036, 2020.

781   Cao, F., Tzortziou, M., Hu, C., Mannino, A., Fichot, C. G., Del Vecchio, R., Najjar, R. G. and Novak, M.:
782   Remote sensing retrievals of colored dissolved organic matter and dissolved organic carbon
783   dynamics in North American estuaries and their margins, Remote Sens. Environ., 205(November
784   2017), 151–165, doi:10.1016/j.rse.2017.11.014, 2018.

785   Chapman, P. M., Hayward, A. and Faithful, J.: Total Suspended Solids Effects on Freshwater Lake
786   Biota Other than Fish, Bull. Environ. Contam. Toxicol., 99(4), 423–427, doi:10.1007/s00128-017-
787   2154-y, 2017.

788   Chen, S., Huang, W., Chen, W. and Chen, X.: An enhanced MODIS remote sensing model for
789   detecting rainfall effects on sediment plume in the coastal waters of Apalachicola Bay, Mar. Environ.
790   Res., 72(5), 265–272, doi:10.1016/j.marenvres.2011.09.014, 2011.

791   Chen, S., Han, L., Chen, X., Li, D., Sun, L. and Li, Y.: Estimating wide range Total Suspended Solids
792   concentrations from MODIS 250-m imageries: An improved method, ISPRS J. Photogramm. Remote
793   Sens., 99, 58–69, doi:10.1016/j.isprsjprs.2014.10.006, 2015a.

Chen, S., Han, L., Chen, X., Li, D., Sun, L. and Li, Y.: Estimating wide range Total Suspended Solids concentrations from MODIS 250-m imageries: An improved method, ISPRS J. Photogramm. Remote Sens., 99, 58–69, doi:10.1016/j.isprsjprs.2014.10.006, 2015b.

Chen, Z., Hu, C. and Muller-karger, F.: Monitoring turbidity in Tampa Bay using MODIS / Aqua 250-m imagery, , 109, 207–220, doi:10.1016/j.rse.2006.12.019, 2007.

Cherukuru, N., Ford, P. W., Matear, R. J., Oubelkheir, K., Clementson, L. A., Suber, K. and Steven, A. D. L.: Estimating dissolved organic carbon concentration in turbid coastal waters using optical remote sensing observations, Int. J. Appl. Earth Obs. Geoinf., 52, 149–154, doi:10.1016/j.jag.2016.06.010, 2016a.

Cherukuru, N., Ford, P. W., Matear, R. J., Oubelkheir, K., Clementson, L. A., Suber, K. and Steven, A. D. L.: Estimating dissolved organic carbon concentration in turbid coastal waters using optical remote sensing observations, Int. J. Appl. Earth Obs. Geoinf., 52, 149–154, doi:10.1016/j.jag.2016.06.010, 2016b.

Cherukuru, N., Martin, P., Sanwlani, N., Mujahid, A. and Müller, M.: A semi-analytical optical remote sensing model to estimate suspended sediment and dissolved organic carbon in tropical coastal waters influenced by peatland-draining river discharges off sarawak, borneo, Remote Sens., 13(1), 1–31, doi:10.3390/rs13010099, 2021.

Chong, X. Y., Gibbins, C. N., Vericat, D., Batalla, R. J., Teo, F. Y. and Lee, K. S. P.: A framework for Hydrological characterisation to support Functional Flows (HyFFlow): Application to a tropical river, J. Hydrol. Reg. Stud., 36(January), doi:10.1016/j.ejrh.2021.100838, 2021.

CIFOR: Forest Carbon Database, [online] Available from: https://carbonstock.cifor.org/, n.d.

Davies, J., Mathhew, U., Aikanathan, S., Nyon, Y. C. and Chong, G.: A Quick Scan of Peatlands, Wetl. Int. Malaysia, 1(March), 1–80, 2010.

Department of Environment: Malaysia Marine Water Quality Standards and Index, , 16 [online] Available from: https://www.doe.gov.my/portalv1/wp-content/uploads/2019/04/BOOKLET-BI.pdf (Accessed 12 September 2021), 2019.

DID: Department of Irrigation & Drainage Sarawak: Introduction to Integrated Coastal Zone Management, [online] Available from: https://did.sarawak.gov.my/page-0-123-476-INTEGRATED-COASTAL-ZONE-MANAGEMENT.html (Accessed 21 October 2021a), 2021.

DID: Department Of Irrigation & Drainage Sarawak, 2021b.

Dindang, A., Chung, C. N. and Seth, S.: Heavy Rainfall Episodes over Sarawak during January-February 2011 Northeast Monsoon, JMM Res. Publ., (11), 41, 2011.

Dogliotti, A. I., Ruddick, K. G., Nechad, B., Doxaran, D. and Knaeps, E.: A single algorithm to retrieve turbidity from remotely-sensed data in all coastal and estuarine waters, Remote Sens. Environ., 156, 157–168, doi:10.1016/j.rse.2014.09.020, 2015.

Donohue, I. and Garcia Molinos, J.: Impacts of increased sediment loads on the ecology of lakes, Biol. Rev., 84(4), 517–531, doi:10.1111/j.1469-185X.2009.00081.x, 2009.

Erftemeijer, P. L. A., Riegl, B., Hoeksema, B. W. and Todd, P. A.: Environmental impacts of dredging and other sediment disturbances on corals: A review, Mar. Pollut. Bull., 64(9), 1737–1765, doi:10.1016/j.marpolbul.2012.05.008, 2012.

Espinoza Villar, R., Martinez, J. M., Le Texier, M., Guyot, J. L., Fraizy, P., Meneses, P. R. and Oliveira, E. de: A study of sediment transport in the Madeira River, Brazil, using MODIS remote-sensing images, J. South Am. Earth Sci., 44, 45–54, doi:10.1016/j.jsames.2012.11.006, 2013.

837 Fabricius, K. E.: Effects of terrestrial runoff on the ecology of corals and coral reefs: Review and
838 synthesis, Mar. Pollut. Bull., 50(2), 125–146, doi:10.1016/j.marpolbul.2004.11.028, 2005.

839 Fabricius, K. E., Logan, M., Weeks, S. J., Lewis, S. E. and Brodie, J.: Changes in water clarity in
840 response to river discharges on the Great Barrier Reef continental shelf: 2002-2013, Estuar. Coast.
841 Shelf Sci., 173, A1–A15, doi:10.1016/j.ecss.2016.03.001, 2016.

842 Gaveau, D. L. A., Sheil, D., Salim, M. A., Arjasakusuma, S., Ancrenaz, M., Pacheco, P. and Meijaard, E.:
843 Rapid conversions and avoided deforestation : examining four decades of industrial plantation
844 expansion in Borneo, Nat. Publ. Gr., (September), 1–13, doi:10.1038/srep32017, 2016.

845 Gilmour, J. P., Cooper, T. F., Fabricius, K. E. and Smith, L. D.: Early warning indicators of change in the
846 condition of corals and coral communities in response to key anthropogenic stressors in the Pilbara,
847 Western Australia, Aust. Inst. Mar. Sci. Rep. to Environ. Prot. Authority. 101pp, 2006.

848 Giuliani, G., Chatenoux, B., Piller, T., Moser, F. and Lacroix, P.: Data Cube on Demand (DCoD):
849 Generating an earth observation Data Cube anywhere in the world, Int. J. Appl. Earth Obs. Geoinf.,
850 87(December 2019), 102035, doi:10.1016/j.jag.2019.102035, 2020.

851 Gomes, V. C. F., Carlos, F. M., Queiroz, G. R., Ferreira, K. R. and Santos, R.: Accessing and Processing
852 Brazilian Earth Observation Data Cubes With the Open Data Cube Platform, ISPRS Ann. Photogramm.
853 Remote Sens. Spat. Inf. Sci., V-4–2021, 153–159, doi:10.5194/isprs-annals-v-4-2021-153-2021, 2021.

854 Gomyo, M. and Koichiro, K.: Spatial and temporal variations in rainfall and the ENSO-rainfall
855 relationship over Sarawak, Malaysian Borneo, Sci. Online Lett. Atmos., 5, 41–44,
856 doi:10.2151/sola.2009-011, 2009.

857 González Vilas, L., Spyrakos, E. and Torres Palenzuela, J. M.: Neural network estimation of
858 chlorophyll a from MERIS full resolution data for the coastal waters of Galician rias (NW Spain),
859 Remote Sens. Environ., 115(2), 524–535, doi:10.1016/j.rse.2010.09.021, 2011.

860 Ha, N. T. T., Thao, N. T. P., Koike, K. and Nhuan, M. T.: Selecting the best band ratio to estimate
861 chlorophyll-a concentration in a tropical freshwater lake using sentinel 2A images from a case study
862 of Lake Ba Be (Northern Vietnam), ISPRS Int. J. Geo-Information, 6(9), doi:10.3390/ijgi6090290,
863 2017.

864 Henley, W. F., Patterson, M. A., Neves, R. J. and Dennis Lemly, A.: Effects of Sedimentation and
865 Turbidity on Lotic Food Webs: A Concise Review for Natural Resource Managers, Rev. Fish. Sci., 8(2),
866 125–139, doi:10.1080/10641260091129198, 2000.

867 Hodgson, G.: Tetracycline reduces sedimentation damage to corals, Mar. Biol., 104(3), 493–496,
868 1990.

869 Hon, J. and Shibata, S.: A Review on Land Use in the Malaysian State of Sarawak, Borneo and
870 Recommendations for Wildlife Conservation Inside Production Forest Environment, Borneo J.
871 Resour. Sci. Technol., 3(2), 22–35, doi:10.33736/bjrst.244.2013, 2013.

872 Horsburgh, J. S., Spackman, A., Stevens, D. K., Tarboton, D. G. and Mesner, N. O.: Environmental
873 Modelling & Software A sensor network for high frequency estimation of water quality constituent
874 fluxes using surrogates, , 25, 1031–1044, doi:10.1016/j.envsoft.2009.10.012, 2010.

875 Howarth, R. W.: Coastal nitrogen pollution: A review of sources and trends globally and regionally,
876 Harmful Algae, 8(1), 14–20, doi:10.1016/j.hal.2008.08.015, 2008.

877 Hu, C., Lee, Z. and Franz, B.: Chlorophyll a algorithms for oligotrophic oceans: A novel approach
878 based on three-band reflectance difference, J. Geophys. Res. Ocean., 117(1), 1–25,
879 doi:10.1029/2011JC007395, 2012.

880   Jiang, D., Matsushita, B., Pahlevan, N., Gurlin, D., Lehmann, M. K., Fichot, C. G., Schalles, J., Loisel, H.,
881   Binding, C., Zhang, Y., Alikas, K., Kangro, K., Uusõue, M., Ondrusek, M., Greb, S., Moses, W. J.,
882   Lohrenz, S. and O'Donnell, D.: Remotely estimating total suspended solids concentration in clear to
883   extremely turbid waters using a novel semi-analytical method, Remote Sens. Environ., 258,
884   doi:10.1016/j.rse.2021.112386, 2021.

885   Jiang, H. and Liu, Y.: Monitoring of TSS concentration in Poyang Lake based on MODIS data, Yangtze
886   River, 42(17), 87–90, 2011.

887   Kemp, P., Sear, D., Collins, A., Naden, P. and Jones, I.: The impacts of fine sediment on riverine fish,
888   Hydrol. Process., 25(11), 1800–1821, doi:10.1002/hyp.7940, 2011.

889   Killough, B.: The Impact of Analysis Ready Data in the Africa Regional Data Cube, Int. Geosci. Remote
890   Sens. Symp., (July 2019), 5646–5649, doi:10.1109/IGARSS.2019.8898321, 2019.

891   Kim, H. C., Son, S., Kim, Y. H., Khim, J. S., Nam, J., Chang, W. K., Lee, J. H., Lee, C. H. and Ryu, J.:
892   Remote sensing and water quality indicators in the Korean West coast: Spatio-temporal structures of
893   MODIS-derived chlorophyll-a and total suspended solids, Mar. Pollut. Bull., 121(1–2), 425–434,
894   doi:10.1016/j.marpolbul.2017.05.026, 2017.

895   Krause, C., Dunn, B., Bishop-Taylor, R., Adams, C., Burton, C., Alger, M., Chua, S., Phillips, C., Newey,
896   V., Kouzoubov, K., Leith, A., Ayers, D., Hicks, A. and DEA Notebooks contributors 2021: Digital Earth
897   Australia notebooks and tools repository, , doi:https://doi.org/10.26186/145234, 2021.

898   Langer, O. E.: Effects of sedimentation on salmonid stream life, Environmental Protection Service.,
899   1980.

900   Lavigne, H., Van der Zande, D., Ruddick, K., Cardoso Dos Santos, J. F., Gohin, F., Brotas, V. and
901   Kratzer, S.: Quality-control tests for OC4, OC5 and NIR-red satellite chlorophyll-a algorithms applied
902   to coastal waters, Remote Sens. Environ., 255, 112237, doi:10.1016/j.rse.2020.112237, 2021.

903   Lee, K. H., Noh, J. and Khim, J. S.: The Blue Economy and the United Nations' sustainable
904   development goals: Challenges and opportunities, Environ. Int., 137(October 2019), 105528,
905   doi:10.1016/j.envint.2020.105528, 2020a.

906   Lee, W. C., Viswanathan, K. K., Kamri, T. and King, S.: Status of Sarawak Fisheries: Challenges and
907   Way Forward, Int. J. Serv. Manag. Sustain., 5(2), 187–200, doi:10.24191/ijsms.v5i2.11719, 2020b.

908   Lemley, D. A., Adams, J. B., Bornman, T. G., Campbell, E. E. and Deyzel, S. H. P.: Land-derived
909   inorganic nutrient loading to coastal waters and potential implications for nearshore plankton
910   dynamics, Cont. Shelf Res., 174(August 2018), 1–11, doi:10.1016/j.csr.2019.01.003, 2019.

911   Lewis, A., Oliver, S., Lymburner, L., Evans, B., Wyborn, L., Mueller, N., Raevksi, G., Hooke, J.,
912   Woodcock, R., Sixsmith, J., Wu, W., Tan, P., Li, F., Killough, B., Minchin, S., Roberts, D., Ayers, D.,
913   Bala, B., Dwyer, J., Dekker, A., Dhu, T., Hicks, A., Ip, A., Purss, M., Richards, C., Sagar, S., Trenham, C.,
914   Wang, P. and Wang, L. W.: The Australian Geoscience Data Cube — Foundations and lessons
915   learned, Remote Sens. Environ., 202, 276–292, doi:10.1016/j.rse.2017.03.015, 2017.

916   Limcih, F., Jilnm, M., Hb, H., Ilcach, H. N. M., Mnl, F., Fi, F. and Nb, F.: Study of Coastal Areas in Miri,
917   in World Engineering Congress 2010, pp. 56–65., 2010.

918   Ling, T. Y., Soo, C. L., Sivalingam, J. R., Nyanti, L., Sim, S. F. and Grinang, J.: Assessment of the Water
919   and Sediment Quality of Tropical Forest Streams in Upper Reaches of the Baleh River, Sarawak,
920   Malaysia, Subjected to Logging Activities, J. Chem., 2016, doi:10.1155/2016/8503931, 2016.

921   Liu, B., D'Sa, E. J. and Joshi, I.: Multi-decadal trends and influences on dissolved organic carbon
922   distribution in the Barataria Basin, Louisiana from in-situ and Landsat/MODIS observations, Remote

923   Sens. Environ., 228(May), 183–202, doi:10.1016/j.rse.2019.04.023, 2019.

924   Loisel, H., Mangin, A., Vantrepotte, V., Dessailly, D., Ngoc Dinh, D., Garnesson, P., Ouillon, S.,
925   Lefebvre, J. P., Mériaux, X. and Minh Phan, T.: Variability of suspended particulate matter
926   concentration in coastal waters under the Mekong's influence from ocean color (MERIS) remote
927   sensing over the last decade, Remote Sens. Environ., 150, 218–230, doi:10.1016/j.rse.2014.05.006,
928   2014.

929   Long, S. M.: Sarawak Coastal Biodiversity : A Current Status, Kuroshio Sci., 8(1), 71–84 [online]
930   Available from: https://www.researchgate.net/publication/265793245, 2014.

931   Lu, Y., Yuan, J., Lu, X., Su, C., Zhang, Y., Wang, C., Cao, X., Li, Q., Su, J., Ittekkot, V., Garbutt, R. A.,
932   Bush, S., Fletcher, S., Wagey, T., Kachur, A. and Sweijd, N.: Major threats of pollution and climate
933   change to global coastal ecosystems and enhanced management for sustainability, Environ. Pollut.,
934   239, 670–680, doi:10.1016/j.envpol.2018.04.016, 2018.

935   Macklin, M. G., Jones, A. F. and Lewin, J.: River response to rapid Holocene environmental change:
936   evidence and explanation in British catchments, Quat. Sci. Rev., 29(13–14), 1555–1576,
937   doi:10.1016/j.quascirev.2009.06.010, 2010.

938   Mao, Z., Chen, J., Pan, D., Tao, B. and Zhu, Q.: A regional remote sensing algorithm for total
939   suspended matter in the East China Sea, Remote Sens. Environ., 124, 819–831,
940   doi:10.1016/j.rse.2012.06.014, 2012.

941   Martin, P., Cherukuru, N., Tan, A. S. Y., Sanwlani, N., Mujahid, A. and Müller, M.: Distribution and
942   cycling of terrigenous dissolved organic carbon in peatland-draining rivers and coastal waters of
943   Sarawak, Borneo, Biogeosciences, 15(22), 6847–6865, doi:10.5194/bg-15-6847-2018, 2018.

944   Mengen, D., Ottinger, M., Leinenkugel, P. and Ribbe, L.: Modeling river discharge using automated
945   river width measurements derived from sentinel-1 time series, Remote Sens., 12(19), 1–24,
946   doi:10.3390/rs12193236, 2020.

947   Mohammad Razi, M. A., Mokhtar, A., Mahamud, M., Rahmat, S. N. and Al-Gheethi, A.: Monitoring of
948   river and marine water quality at Sarawak baseline, Environ. Forensics, 22(1–2), 219–240,
949   doi:10.1080/15275922.2020.1836076, 2021.

950   Morel, A. and Bélanger, S.: Improved detection of turbid waters from ocean color sensors
951   information, Remote Sens. Environ., 102(3–4), 237–249, doi:10.1016/j.rse.2006.01.022, 2006.

952   Morel, A. and Gentili, B.: A simple band ratio technique to quantify the colored dissolved and detrital
953   organic material from ocean color remotely sensed data, Remote Sens. Environ., 113(5), 998–1011,
954   doi:10.1016/j.rse.2009.01.008, 2009.

955   Mueller, J., Mueller, J., Pietras, C., Hooker, S., Clark, D., Frouin, A., Mitchell, B., Bidigare, R., Trees, C.
956   and Werdell, J.: Ocean Optics Protocols For Satellite Ocean Color Sensor Validation, Revision 3,
957   volumes 1 and 2., 2002.

958   Müller-dum, D., Warneke, T., Rixen, T., Müller, M., Baum, A., Christodoulou, A., Oakes, J., Eyre, B. D.
959   and Notholt, J.: Impact of peatlands on carbon dioxide (CO 2) emissions from the Rajang River and
960   Estuary , Malaysia, , 17–32, 2019.

961   Müller, D., Warneke, T., Rixen, T., Müller, M., Mujahid, A., Bange, H. W. and Notholt, J.: Fate of
962   terrestrial organic carbon and associated CO2 and CO emissions from two Southeast Asian estuaries,
963   Biogeosciences, 13(3), 691–705, doi:10.5194/bg-13-691-2016, 2016.

964   NASA Official: Ocean Level-2 Data Format Specification, [online] Available from:
965   https://oceancolor.gsfc.nasa.gov/docs/format/l2nc/, n.d.

966 Nazirova, K., Alferyeva, Y., Lavrova, O., Shur, Y., Soloviev, D., Bocharova, T. and Strochkov, A.:
967 Comparison of in situ and remote-sensing methods to determine turbidity and concentration of
968 suspended matter in the estuary zone of the mzymta river, black sea, Remote Sens., 13(1), 1–29,
969 doi:10.3390/rs13010143, 2021.

970 Neil, C., Spyrakos, E., Hunter, P. D. and Tyler, A. N.: A global approach for chlorophyll-a retrieval
971 across optically complex inland waters based on optical water types, Remote Sens. Environ.,
972 229(May), 159–178, doi:10.1016/j.rse.2019.04.027, 2019.

973 Omorinoye, O. A., Assim, Z. Bin and Jusoh, I. Bin: Geomorphological and Sedimentological Features
974 of River Sadong, Sarawak, Malaysia, Indones. J. Geosci., 8(1), 119–130, doi:10.17014/ijog.8.1.119-
975 130, 2021.

976 Ondrusek, M., Stengel, E., Kinkade, C. S., Vogel, R. L., Keegstra, P., Hunter, C. and Kim, C.: The
977 development of a new optical total suspended matter algorithm for the Chesapeake Bay, Remote
978 Sens. Environ., 119, 243–254, doi:10.1016/j.rse.2011.12.018, 2012.

979 Open Data Cube: Open Data Cube, [online] Available from:
980 https://opendatacube.readthedocs.io/en/latest/user/intro.html (Accessed 25 October 2021), 2021.

981 Park, G. S.: The role and distribution of total suspended solids in the macrotidal coastal waters of
982 Korea, Environ. Monit. Assess., 135(1–3), 153–162, doi:10.1007/s10661-007-9640-3, 2007.

983 Petus, C., Marieu, V., Novoa, S., Chust, G., Bruneau, N. and Froidefond, J. M.: Monitoring spatio-
984 temporal variability of the Adour River turbid plume (Bay of Biscay, France) with MODIS 250-m
985 imagery, Cont. Shelf Res., 74, 35–49, doi:10.1016/j.csr.2013.11.011, 2014.

986 Praveena, S. M., Siraj, S. S. and Aris, A. Z.: Coral reefs studies and threats in Malaysia: A mini review,
987 Rev. Environ. Sci. Biotechnol., 11(1), 27–39, doi:10.1007/s11157-011-9261-8, 2012.

988 Ramaswamy, V., Rao, P. S., Rao, K. H., Thwin, S., Rao, N. S. and Raiker, V.: Tidal influence on
989 suspended sediment distribution and dispersal in the northern Andaman Sea and Gulf of Martaban,
990 Mar. Geol., 208(1), 33–42, doi:10.1016/j.margeo.2004.04.019, 2004.

991 Refaeilzadeh, P., Tang, L., Liu, H., Angeles, L. and Scientist, C. D.: Encyclopedia of Database Systems,
992 Encycl. Database Syst., doi:10.1007/978-1-4899-7993-3, 2020.

993 Risk, M. J. and Edinger, E.: Impacts of sediment on coral reefs, Encycl. Mod. coral reefs. Springer,
994 Netherlands, 575–586, 2011.

995 Rogers, C. S.: The effect of shading on coral reef structure and function, J. Exp. Mar. Bio. Ecol., 41(3),
996 269–288, doi:10.1016/0022-0981(79)90136-9, 1979.

997 Sa'adi, Z., Shahid, S., Chung, E. S. and Ismail, T. bin: Projection of spatial and temporal changes of
998 rainfall in Sarawak of Borneo Island using statistical downscaling of CMIP5 models, Atmos. Res.,
999 197(November 2016), 446–460, doi:10.1016/j.atmosres.2017.08.002, 2017.

1000 Sandifer, P. A., Keener, P., Scott, G. I. and Porter, D. E.: Oceans and Human Health and the New Blue
1001 Economy, Elsevier Inc., 2021.

1002 Seegers, B. N., Stumpf, R. P., Schaeffer, B. A., Loftin, K. A. and Werdell, P. J.: Performance metrics for
1003 the assessment of satellite data products: an ocean color case study, Opt. Express, 26(6), 7404,
1004 doi:10.1364/oe.26.007404, 2018.

1005 Shaw, E. Al and Richardson, J. S.: Direct and indirect effects of sediment pulse duration on stream
1006 invertebrate assemblages and rainbow trout (Oncorhynchus mykiss) growth and survival, Can. J.
1007 Fish. Aquat. Sci., 58(11), 2213–2221, doi:10.1139/f01-160, 2001.

1008   Sim, C., Cherukuru, N., Mujahid, A., Martin, P., Sanwlani, N., Warneke, T., Rixen, T., Notholt, J. and
1009   Müller, M.: A new remote sensing method to estimate river to ocean DOC flux in peatland
1010   dominated Sarawak coastal regions, Borneo, Remote Sens., 12(20), 1–13, doi:10.3390/rs12203380,
1011   2020.

1012   Siswanto, E., Tang, J. and Yamaguchi, H.: Empirical ocean-color algorithms to retrieve chlorophyll- a ,
1013   total suspended matter , and colored dissolved organic matter absorption coefficient in the Yellow
1014   and East China Seas, , 627–650, doi:10.1007/s10872-011-0062-z, 2011.

1015   Slonecker, E. T., Jones, D. K. and Pellerin, B. A.: The new Landsat 8 potential for remote sensing of
1016   colored dissolved organic matter (CDOM), Mar. Pollut. Bull., 107(2), 518–527,
1017   doi:10.1016/j.marpolbul.2016.02.076, 2016.

1018   Song, C., Wang, G., Sun, X., Chang, R. and Mao, T.: Control factors and scale analysis of annual river
1019   water, sediments and carbon transport in China, Sci. Rep., 6(May), 1–14, doi:10.1038/srep25963,
1020   2016.

1021   Song, Z., Shi, W., Zhang, J., Hu, H., Zhang, F. and Xu, X.: Transport mechanism of suspended
1022   sediments and migration trends of sediments in the central hangzhou bay, Water (Switzerland),
1023   12(8), doi:10.3390/W12082189, 2020.

1024   Soo, C. L., Chen, C. A. and Mohd-Long, S.: Assessment of Near-Bottom Water Quality of
1025   Southwestern Coast of Sarawak, Borneo, Malaysia: A Multivariate Statistical Approach, J. Chem.,
1026   2017, doi:10.1155/2017/1590329, 2017.

1027   Soum, S., Ngor, P. B., Dilts, T. E., Lohani, S., Kelson, S., Null, S. E., Tromboni, F., Hogan, Z. S., Chan, B.
1028   and Chandra, S.: Spatial and long-term temporal changes in water quality dynamics of the tonle sap
1029   ecosystem, Water (Switzerland), 13(15), doi:10.3390/w13152059, 2021.

1030   Staub, J. R., Among, H. L. and Gastaldo, R. A.: Seasonal sediment transport and deposition in the
1031   Rajang River delta, Sarawak, East Malaysia, Sediment. Geol., 133(3–4), 249–264, doi:10.1016/S0037-
1032   0738(00)00042-7, 2000.

1033   Sun, C.: Riverine influence on ocean color in the equatorial South China Sea, Cont. Shelf Res.,
1034   143(December 2015), 151–158, doi:10.1016/j.csr.2016.10.008, 2017a.

1035   Sun, C.: Riverine influence on ocean color in the equatorial South China Sea, Cont. Shelf Res.,
1036   143(October 2016), 151–158, doi:10.1016/j.csr.2016.10.008, 2017b.

1037   Sutherland, A. B. and Meyer, J. L.: Effects of increased suspended sediment on growth rate and gill
1038   condition of two southern Appalachian minnows, Environ. Biol. Fishes, 80(4), 389–403,
1039   doi:10.1007/s10641-006-9139-8, 2007.

1040   Swain, R. and Sahoo, B.: Mapping of heavy metal pollution in river water at daily time-scale using
1041   spatio-temporal fusion of MODIS-aqua and Landsat satellite imageries, J. Environ. Manage., 192, 1–
1042   14, doi:10.1016/j.jenvman.2017.01.034, 2017.

1043   Tangang, F. T., Juneng, L., Salimun, E., Sei, K. M., Le, L. J. and Muhamad, H.: Climate change and
1044   variability over Malaysia: Gaps in science and research information, Sains Malaysiana, 41(11), 1355–
1045   1366, 2012.

1046   Tawan, A. S., Ling, T. Y., Nyanti, L., Sim, S. F., Grinang, J., Soo, C. L., Lee, K. S. P. and Ganyai, T.:
1047   Assessment of water quality and pollutant loading of the Rajang River and its tributaries at Pelagus
1048   area subjected to seasonal variation and river regulation, Environ. Dev. Sustain., 22(5), 4101–4124,
1049   doi:10.1007/s10668-019-00374-9, 2020.

1050   Telesnicki, G. J. and Goldberg, W. M.: CORAL REEF PAPER EFFECTS OF TURBIDITY ON THE

1051 PHOTOSYNTHESIS AND RESPIRATION OF TWO SOUTH FLORIDA REEF CORAL SPECIES portant factors
1052 in the regulation of coral cover , diversity , and abundance (Ed- ships between suspended sediment
1053 concentrations or parti, , 57(2), 527–539, 1995.

1054 Tilburg, C. E., Jordan, L. M., Carlson, A. E., Zeeman, S. I. and Yund, P. O.: The effects of precipitation,
1055 river discharge, land use and coastal circulation on water quality in coastal Maine, R. Soc. Open Sci.,
1056 2(7), doi:10.1098/rsos.140429, 2015.

1057 Tromboni, F., Dilts, T. E., Null, S. E., Lohani, S., Ngor, P. B., Soum, S., Hogan, Z. and Chandra, S.:
1058 Changing land use and population density are degrading water quality in the lower mekong basin,
1059 Water (Switzerland), 13(14), 1–16, doi:10.3390/w13141948, 2021.

1060 United Nations: The Ocean Conference, in The Ocean Conference, vol. 53, p. 130, New York., 2017.

1061 Valerio, A. de M., Kampel, M., Vantrepotte, V., Ward, N. D., Sawakuchi, H. O., Less, D. F. D. S., Neu,
1062 V., Cunha, A. and Richey, J.: Using CDOM optical properties for estimating DOC concentrations and
1063 pCO 2 in the Lower Amazon River , Opt. Express, 26(14), A657, doi:10.1364/oe.26.00a657, 2018.

1064 Verschelling, E., van der Deijl, E., van der Perk, M., Sloff, K. and Middelkoop, H.: Effects of discharge,
1065 wind, and tide on sedimentation in a recently restored tidal freshwater wetland, Hydrol. Process.,
1066 31(16), 2827–2841, doi:10.1002/hyp.11217, 2017.

1067 Vijith, H., Hurmain, A. and Dodge-Wan, D.: Impacts of land use changes and land cover alteration on
1068 soil erosion rates and vulnerability of tropical mountain ranges in Borneo, Remote Sens. Appl. Soc.
1069 Environ., 12(September), 57–69, doi:10.1016/j.rsase.2018.09.003, 2018.

1070 Wang, C., Chen, S., Li, D., Wang, D., Liu, W. and Yang, J.: A Landsat-based model for retrieving total
1071 suspended solids concentration of estuaries and coasts in China, Geosci. Model Dev., 10(12), 4347–
1072 4365, doi:10.5194/gmd-10-4347-2017, 2017.

1073 Wang, J., Tong, Y., Feng, L., Zhao, D., Zheng, C. and Tang, J.: Satellite-Observed Decreases in Water
1074 Turbidity in the Pearl River Estuary: Potential Linkage With Sea-Level Rise, J. Geophys. Res. Ocean.,
1075 126(4), 1–17, doi:10.1029/2020JC016842, 2021.

1076 Weber, M., Lott, C. and Fabricius, K. E.: Sedimentation stress in a scleractinian coral exposed to
1077 terrestrial and marine sediments with contrasting physical, organic and geochemical properties, J.
1078 Exp. Mar. Bio. Ecol., 336(1), 18–32, doi:10.1016/j.jembe.2006.04.007, 2006.

1079 Werdell, P. J., McKinna, L. I. W., Boss, E., Ackleson, S. G., Craig, S. E., Gregg, W. W., Lee, Z.,
1080 Maritorena, S., Roesler, C. S., Rousseaux, C. S., Stramski, D., Sullivan, J. M., Twardowski, M. S.,
1081 Tzortziou, M. and Zhang, X.: An overview of approaches and challenges for retrieving marine
1082 inherent optical properties from ocean color remote sensing, Prog. Oceanogr., 160, 186–212,
1083 doi:10.1016/j.pocean.2018.01.001, 2018.

1084 Whitmore, T. C.: Tropical rain forests of the Par East, Oxford. Clarendon Press., 1984.

1085 Wilber, D. H. and Clarke, D. G.: Biological Effects of Suspended Sediments: A Review of Suspended
1086 Sediment Impacts on Fish and Shellfish with Relation to Dredging Activities in Estuaries, North Am. J.
1087 Fish. Manag., 21(4), 855–875, doi:10.1577/1548-8675(2001)021<0855:beossa>2.0.co;2, 2001.

1088 World Bank and United Nations Department of Economic and Social Affairs (UNDESA): The Potential
1089 of the Blue Economy: Increasing Long-term Benefits of the Sustainable Use of Marine Resources for
1090 Small Island Developing States and Coastal Least Developed Countries, World Bank, Washington DC.,
1091 2017.

1092 Wu, C. S., Yang, S. L. and Lei, Y. ping: Quantifying the anthropogenic and climatic impacts on water
1093 discharge and sediment load in the Pearl River (Zhujiang), China (1954-2009), J. Hydrol., 452–453,

1094   190–204, doi:10.1016/j.jhydrol.2012.05.064, 2012.

1095   Yang, S. L., Zhao, Q. Y. and Belkin, I. M.: Temporal variation in the sediment load of the Yangtze river
1096   and the influences of human activities, J. Hydrol., 263(1–4), 56–71, doi:10.1016/S0022-
1097   1694(02)00028-8, 2002.

1098   Zhan, W., Wu, J., Wei, X., Tang, S. and Zhan, H.: Spatio-temporal variation of the suspended
1099   sediment concentration in the Pearl River Estuary observed by MODIS during 2003–2015, Cont. Shelf
1100   Res., 172(May 2018), 22–32, doi:10.1016/j.csr.2018.11.007, 2019.

1101   Zhang, L. J., Wang, L., Cai, W. J., Liu, D. M. and Yu, Z. G.: Impact of human activities on organic carbon
1102   transport in the Yellow River, Biogeosciences, 10(4), 2513–2524, doi:10.5194/bg-10-2513-2013,
1103   2013.

1104   Zhang, M., Tang, J., Dong, Q., Song, Q. T. and Ding, J.: Retrieval of total suspended matter
1105   concentration in the Yellow and East China Seas from MODIS imagery, Remote Sens. Environ.,
1106   114(2), 392–403, doi:10.1016/j.rse.2009.09.016, 2010a.

1107   Zhang, Y., Lin, S., Liu, J., Qian, X. and Ge, Y.: Time-series MODIS image-based retrieval and
1108   distribution analysis of total suspended matter concentrations in Lake Taihu (China), Int. J. Environ.
1109   Res. Public Health, 7(9), 3545–3560, doi:10.3390/ijerph7093545, 2010b.

1110   Zhou, Y., Xuan, J. and Huang, D.: Tidal variation of total suspended solids over the Yangtze Bank
1111   based on the geostationary ocean color imager, Sci. China Earth Sci., 63(9), 1381–1389,
1112   doi:10.1007/s11430-019-9618-7, 2020.

1113

1114

1115

1116

1117

1118

1119

1120

1121

1122

1123

1124

1125

1126

1127

1128

1129